Versatile Separation and Analysis of Heparan Sulfate Oligosaccharides using Graphitised Carbon Liquid Chromatography and Electrospray Mass Spectrometry

Rebecca L. Miller[1,3], Scott E. Guimond[1], Mark Prescott[1], Jeremy E. Turnbull[1]* and Niclas Karlsson[2]*.

[1]Centre for Glycobiology, Department of Biochemistry, Institute of Integrative Biology, University of Liverpool, Crown Street, Liverpool, L69 7ZB, England, UK;

[2]Department of Medical Biochemistry and Cell Biology, Institute of Biomedicine, Sahlgrenska Academy, University of Gothenburg, Box 440, 40530 Gothenburg, Sweden.

[3]Univeristy Of Oxford, Oncology Department, Old Road Campus Research Building, Oxford, OX3 7DQ

*Joint senior author

Authors email address: rebecca.miller@oncology.ox.ac.uk

Corresponding Authors;

Rebecca L. Miller

Email address: rebecca.miller@oncology.ox.ac.uk

Prof. Jeremy Turnbull

Email address: j.turnbull@liverpool.ac.uk

Abstract

Heparin and heparan sulfate (HS) by nature contain multiple isomeric structures, which are fundamental for the regulation of biological processes. Here we report the use of a porous

graphitised carbon (PGC) LC-MS method with effective separation and sensitivity to separate mixtures of digested HS oligosaccharides. Application of this method allowed the separation of oligosaccharide mixtures with various degree of polymerization (dp) ranging from dp4 to dp8, two dp4 isomers that were baseline resolved, four dp6 isomers and the observation of a dp3 oligosaccharides. PGC LC-MS of complex mixtures demonstrated that compounds eluted from the column in decreasing order of hydrophilicity, with the more highly sulfated structures eluting first. Our data indicates that sulfation levels, chain length and conformation all effect elution order. We found that PGC's resolving capabilities of the dp4 and dp6 isomeric structures makes this methodology particularly useful for the sequencing of HS saccharides, since the lack of contaminating isomeric structures provides unambiguous structural assignments from the MS/MS data. Collectively this work demonstrates that PGC column-based methods are powerful tools for enhanced separation and analysis of heterogeneous mixtures of HS saccharide species.

Introduction

Heparin and HS are composed of repeating disaccharide units, containing an alternating arrangement of an uronic acid sugar (either glucuronic or iduronic acid) and a glucosamine residue. The uronic acid residue can be O-sulfated at the carbon 2 position, whereas the glucosamine can be 6-O-sulfated and rarely 3-O-sulfated; in addition, the N-position can be occupied by a sulfate, acetate or un-modified. During biosynthesis these modifications are incomplete, resulting in complex cell and tissue-specific variations in the structural patterns generated, including isomeric structures[1-3]. This variability is responsible for the protein regulatory properties of HS and has been the focus of recent research[4-6]. This complexity also

gives rise to significant challenges for the separation and sequencing of saccharides derived from HS.

Various methods for separation of HS saccharides by chromatography have been developed, however, isolation of a pure saccharide with a single, defined structure is still challenging. Often, size exclusion chromatography (SEC) is the initial methodology used, to produce size defined separations typically aimed at isolating structures with similar numbers of monosaccharide units (degree of polymerization, dp). SEC has also been coupled with mass spectrometry to profile each fraction[1, 7-8]. Since HS saccharides are predominantly negatively charged, SAX (strong anion exchange) and VSCTA (volatile salt cetyltrimethylammonium)-SAX are chromatography methods with the highest resolving power for heparin and HS separation and are often used in tandem to achieved greater resolution[9-10]. However, neither chromatography method is compatible with LC-MS[11].

Reverse phase ion pairing (RP-IP) chromatography, commonly used for protein[12] and peptide[13] separation, has also been effectively utilized for HS saccharides through the addition of an ion pairing agent, such as triethylamine[14-15]. RP-IP provides the resolution and separation allowing it to be the first method to be coupled with MS, enabling LC-MS analysis of HS oligosaccharides[16]. However, a drawback of this method is that the ion-pairing reagent causes signal suppression and ion source contamination. Hydrophilic interaction liquid chromatography (HILIC) is the most recent method to be applied, separating on the basis of hydrophilicity. Since HS is a particularly hydrophilic molecule with multiple polar side groups (sulfates, carboxylates and hydroxyls), HILIC is a good choice for the separation of these compounds. It has been used in both offline and online modes to separate a wide range of structures including *O*-glycans[17], *N*-glycans[18], GAG disaccharides[19] and GAG oligosaccharides[20-21]. HILIC is also the most recent

technique to be coupled with MS for these applications[22-23]; although it lacks the resolution of SAX and RP-IP, it has higher sensitivity and is MS compatible.

PGC has been used for decades in the analysis of small oligosaccharides, in particular *O*-linked glycans[24] and *N*-linked glycans[25-26].The hydrophobic attributes of graphite mean that the columns behave in a similar manner to reverse phase material; the electronic properties are due to the polarizable surface causing a charge-induced dipole with the retention of negatively charged molecules[27]. PGC can act as both an oxidising and reducing reagent towards analytes, whereby its current state can affect the retention time and peak shape of the separated analytes. Altered analyte retention generally results from PGC contamination, thus requiring regular backflush with strong acids / bases and solvents (tetrahydrofuran, acetone, trifluoroacetate, hydrochloric acid and sodium hydroxide) as part of normal maintance[28-29]. Graphite can retain many glycan structures, and has been demonstrated to have high resolving capacity including separating α and β anomers[26, 30-31]. The main advantage of this technique is that it uses volatile buffers, usually in the presence of acetonitrile and so can be readily coupled with MS. This has also been shown to effectively separate charged oligosaccharides, such a chondroitin sulfate[32], keratan sulfate, heparin and HS disaccharides[30].

Here, we describe for the first time the separation of HS oligosaccharide digests by PGC LC-MS. The low concentration of volatile ammonium bicarbonate causes little source contamination, increased ion sensitivity and sulfate protection[33]. Our data highlights the advantages of PGC LC-MS for separation and purification of complex mixtures of HS oligosaccharides (including isomeric structures) with good sensitivity, establishing this methodology as a valuable tool for HS analysis.

Experimental

Materials and Reagents. Porcine mucosal heparan sulfate (PMHS) (Celsus Laboratories, Cincinnati, OH) was digested with recombinant heparinase III obtained from IBEX Technologies (Montreal, Canada). HPLC-grade water (Chromasolv, VWR, Radnor, Pennsylvania) was used throughout. All other reagents were of HPLC grade (Sigma-Aldrich, St Louis, MO).

Depolymerisation of HS: Heparan sulfate (50 mg) was reconstituted in 300 µl of lyase buffer (100 mM sodium acetate, 10 mM calcium acetate), and digested using 120 mU of heparinase III for 24 hrs at 37 ^{o}C.

SEC separation. SEC separations were performed on an Äkta P-900 FPLC system (GE Healthcare, Buckinghamshire, UK) using a XK16 column packed with Superdex 30 (30 mm x 200 cm, bead size 34µm) using UV-spectrophotometric detection at 232 nm. Digested PMHS (50 mg/ml, 1.0 ml) was injected onto the column and separated using 0.5 M ammonium bicarbonate eluent at a flow rate of 0.5 ml/min. Fractions (0.5 ml) from each peak were pooled and repeatedly freeze dried using water until all the ammonium bicarbonate was lyophilized.

Strong Anion-Exchange Chromatography (SAX). SAX separations were performed on a Shimadzu SPD 10A system (Manchester, UK) with a Propac PA1 column (4.6 mm x 250 mm, 5 µm bead size (Thermo Scientific, Waltham, Massachusetts), with a UV-visible spectrophotometric detector. Eluent A was HPLC grade water and eluent B was 2.0 M NaCl. The elution profiles were monitored with an absorbance at 232 nm. A 2 mg dp4 SEC fraction was injected, and eluted with a linear gradient of 0-70 % B in A over 120 mins using a flow rate of 1 ml/min at a temperature of 40 ^{o}C.

PGC on-line mass spectrometry using an ion trap instrument.

Online LC-MS was performed using an Agilent Technologies 1100 series LC system coupled to an Agilent Technologies MSD-XCT Plus Ion Trap mass spectrometer (Agilent Technologies, Palo Alto CA). Eluent A was HPLC grade water with 10 mM ammonium bicarbonate, eluent B was 80 % acetonitrile with 10 mM ammonium bicarbonate and eluent C HPLC grade water, 0.1 % acetic acid. The porous graphitised carbon Protecol capillary column (100 x 0.32 mm, 5 µm, SGE, Melbourne, Australia) was equilibrated in eluent A and samples of varying concentrations were injected and subjected to a linear gradient 0-40 % B in A (v/v) over 40 minutes at a flow rate of 4 µl/min. The column was regenerated with a 10 min wash cycle using 100 % eluent C followed by equilibration in eluent A (10 min). Elution into the ESI electrospray source was achieved at a flow rate of 4 µl $min^{-1}$and heated to 270 ^{o}C. The negative ion mass spectrum of the sample was recorded using a spray voltage of 3.5 kV. The PGC column was left in buffer B overnight and between runs.

PGC on-line mass spectrometry using a Q-TOF instrument.

Online LC-MS of Arixtra was performed using a Waters Q-TOF Micro (Manchester, UK). Eluent A was HPLC grade water with 20 mM ammonium bicarbonate, eluent B was 80 % acetonitrile with 20 mM ammonium bicarbonate and eluent C was HPLC grade water, 0.1 % acetic acid. The porous graphitised carbon Hypercarb column (100 mm x 4.6 mm, 5 µm) was equilibrated in eluent A and samples of varying concentrations were injected and subjected to a linear gradient 0-40 % B in A (v/v) over 40 minutes at a flow rate of 0.3 ml/min. The column was regenerated with a 10 min wash cycle using 100 % eluent C followed by equilibration in eluent A (10 min). Elution into the ESI electrospray source was achieved at a flow rate of 300 µl min^{-1} and heated to 270 ^{o}C. The negative ion mass spectrum of the sample was recorded using a spray voltage of 2200 V. The PGC column was left in buffer B overnight and between runs.

Off-line mass spectrometry. Each sample was infused into the nano-electrospray source of the mass spectrometer (Waters Q-TOF Micro, Manchester, UK) at a flow rate of 50 µl h^{-1}, via a 1 µm tip. The negative ion mass spectrum of the sample was recorded using a spray voltage at 2200 V, sample voltage at 20V, extraction cone voltage at 1 V and collision energy at 3 V. Each sample was at a final concentration of 5 pmol/µl in water/acetonitrile (50:50, v/v). MS/MS was performed on selected masses, using the same conditions with the exception of the collision energy, which ranged from 3 V – 30 V.

Data Interpretation. Glycoworkbench was used to create schematic oligosaccharide structures. A manually generated spreadsheet file (excel) of each structure was calculated for 1 glycosidic bond cleavage and validated with an example structure using Glycoworkbench. GWP files were exported from Glycoworkbench and submitted with Agilent file exported peak lists of generated data to the UniCarb-DB database (available in next version at http://unicarb-db.org/references/342).

Results and Discussion

Initial separation of HS digested oligosaccharides.

PMHS was digested using heparinase III and its oligosaccharide products were separated by preparative scale SEC on a Superdex 30 column (Figure S-1)[11]. Fractions corresponding to each peak were collected and subjected to a brief screening by offline MS (data not shown) to ascertain the average size of its constituent saccharides, calculated from the two most intense ions. Selected SEC fractions were either subject to PGC LC-MS as oligosaccharide mixtures or further purified through SAX and then subjected to PGC LC-MS as demonstrated in the workflow in Figure 1. Previous studies demonstrated the utility of PGC LC-MS for examining

HS disaccharides[30]. Chromatography and LC-MS methodologies have been used to identify HS disaccharide changes in disease models[34-35]. However, biological information gained from disaccharide analysis is limited, since longer HS oligosaccharides are required to incur biological effects[23, 36-37]. To get insight into these larger oligosaccharides, PGC LC-MS was used to separate SEC oligosaccharide fractions (Base peak chromatograms in Figures 2a, 2b, and 2c) and Arixtra (Figure S-2). Each ion from the SEC fractions was identified using the combinatorial generated database of possible dp4, dp6 and dp8 (Tables S-1, S-2, and S-3) generated using Glycoworkbench[38] and relative oligosaccharide abundances are displayed as bar charts (Figures S-3 to S-6). SEC peak A (Figure S-1) contained dp4's with 3-4 sulfate groups, dp6's with 0-4 sulfate groups and a dp8 with 0 sulfate groups (Figure 2a, Table S-1 and Figure S-3). SEC peak B (Figure S-1) contained dp6's with 1-5 sulfate groups and dp8's with 0-2 sulfate groups (Figure 2b, Table S-2 and Figure S-4). SEC peak C contained dp6's with 3-5 sulfate groups and dp8's with 0-5 sulfate groups (Figure 2c, Table S-3 and Figure S-5). Analysis of each SEC fraction did show low abundant oligosaccharides containing the rare free amines, which could either be a result of heparin processing or part of the native structure. A characteristic of the graphite column for oligosaccharide separation and elution is hydrophilicity. It was observed that higher levels of sulfation within each dp eluted earlier than lower levels. Analysis of identified ions from each fraction indicated that PGC provided isomeric separation of heparan sulfate oligosaccharides, which was further evaluated.

Analysis of dp4 HS saccharides by PGC LC-MS.

A dp4 SEC fraction (Figure S-1, peak A) was subjected to further orthogonal separation by SAX ProPac PA1 chromatography (Figure S-7). Two peaks, D and E (Figure S-7) were selected for

analysis via PGC LC-MS to determine their structural sequence and purity. LC-MS of peak D displayed two peaks (peaks F and G) both with an $[M - H]^-$ of *m/z* 795 (Figures 3a and 3b) corresponding to a dp4 + 1Ac + $1SO_3$. MS/MS performed on the parent ions from the isomers generated unique product ion spectra for oligosaccharide sequencing (Figures 3c and 3d). Only two sequence combinations for *m/z* 795 $[M - H]^-$ exist; ΔUA – GlcN**S** – UA – GlcNAc and ΔUA – GlcNAc – UA – GlcN**S**, both showing different signal intensities of B, Y, C and Z product ions (Figures 3d and 3e). Each structure was deduced from these fragments (with only one cross ring cleavage and no sulfation loss) (Tables S-5 and S-6). Structure F, eluting at 18 minutes, displays a large proportion of B, Y, C and Z ions corresponding to the sequence ΔUA – GlcN**S** – UA – GlcNAc (Table S-5 and Figure 3c), whereas, structure G, eluting at 21 minutes, displays B, Y, C and Z ions of the structure ΔUA – GlcNAc – UA – GlcN**S** (Table S-6 and Figure 3d). Although both oligosaccharides have some isomeric product ions, the ions B_3 (*m/z* 574), and Y_2 (*m/,* 396) are unique to peak F (Figure 3c and Table S-5) and B_3, (*m/z* 536), Y_1 (*m/z* 258), and C_3 (*m/z* 554) are unique to peak G (Figure 3d and Table S-6). Baseline resolution observed in two isomeric oligosaccharide structures proved the capability and the value of PGC LC-MS. LC-MS/MS of SAX separated peak E (Figure S-2) displayed a single peak (PGC - peak H) with an $[M-2H]^{2-}$ of *m/z* 477 (Figure 3b) corresponding to a dp4 + 1Ac + $3SO_3$, which has 12 theoretical isomeric structures (Tables S-7 to S-18). The MS/MS performed on peak H (Figure 3e) showed the product ions B_1 (*m/z* 157), B_2 (*m/z* 398), B_3 (*m/z* 654), C_2 (*m/,* 416), Y_1 (*m/z* 300), Z_1 (*m/z* 282), Z_2 (*m/z* 538) and Z_3 (*m/z* 779) represented nearly a full set of B, Y, C and Z ions concluding that the structure has the sequence of ΔUA – GlcN**S** – UA2**S** – GlcNAc6**S** (Table S-7 and Figure 3e). All products ions were assigned using Domon and Costello nomenclature[39].

Separation of dp6 HS structures using PGC LC-MS

Isomeric structures are a prominent feature in HS, due to characteristic repeating disaccharide units with multiple locations for sulfate group modifications. The close chemical resemblance between HS oligosaccharide isomers provides a separation challenge for columns currently used for this application. Columns that have the greatest resolving capabilities require high levels of salt incompatible with LC-MS. Therefore, a tandem separation approach is advantageous, where the last step would be a low salt high resolution LC-MS method. To investigate the isomeric separation capabilities of PGC, a complex SEC dp6 mixture was subjected to PGC LC-MS analysis. The EIC (extracted ion chromatogram) of $[M - 2H]^{2-}$ ion of *m/z* 645.5 corresponding to a dp6 + 1Ac + $3SO_3$ from fraction B (SEC separation Figure S-1 and base peak chromatogram from PGC LC-MS in Figure 2b), showed the separation of four of isomeric structures (Figure 4a). The MS/MS spectra performed on each structure indicated that they were different isomers (Figures 4b–4e), where each fragment spectrum showed different signal intensities of B, Y, C and Z product ions (Figures 4b-4e). To interpret the spectra we used biosynthetic rules to build a virtual library (Tables S-19 to S-37). It must therefore consist of one UA – GlcNAc, and two UA – GlcNS, and one additional O-sulfate, as free amines would be only be observed in low abundant structures. With these constraints 18 structures are possible for a single sulfate position, excluding differences in glucuronic and iduronic acid, and the rare free amine and 3-O-sulfate. Only intact product ions (no sulfate loss) were taken into consideration as these were the most informative (Tables S-19 to S-37). Fragment ions represented in Tables S-19 to S-37 are only of a single glycosidic cleavage. However, by having two glycosidic cleavages present it was possible to obtain nearly all product ions for all oligosaccharide sequences, albeit with varying intensities for isomeric structures[40]. Therefore, the assumption was made that a single glycosidic

cleavage would was more likely than internal glycosidic bond fragments. Although it should be noted that this may not always be the case, with some understanding that N-sulfation can be prone to cross-ring cleavage[41-45]. Based on this information the oligosaccharide sequence eluting at 18 mins is ΔUA2**S** - GlcN**S** - UA - GlcN**S** - UA - GlcNAc (Figure 4b, Table S-19). Close to a full set of Y ions; Y_2 (*m/z* 396) (UA – GlcNAc), Y_3 (*m/z* 637) (GlcNS – UA – GlcNAc), Y_4 (*m/z* 813) (UA – GlcNS – UA – GlcNAc) and Y_5 (*m/z* 526) (GlcNS – UA – GlcNS – UA – GlcNAc) were observed, with some complementary B and C ions; B_2 (*m/z* 478) (ΔUA2S – GlcNS), C_2 (*m/z* 496) (ΔUA2S – GlcNS –) and B_4 (*m/z* 447) (ΔUA2S – GlcNS – UA – GlcNS). The interpretation of the oligosaccharide eluting at 20 mins with 6 assigned fragment ions indicated that this was a mixture of two isomers in that peak. What appeared to be the dominating isomer was the ΔUA2**S** – GlcN**S** – UA – GlcNAc – UA – GlcN**S** structure based on the fragments Y_3 (*m/z* 637) (GlcNAc – UA – GlcNS), Y_5 (*m/z* 526) (GlcNS – UA – GlcNAc – UA – GlcNS), Z_2 (*m/z* 416) (UA – GlcNS), Z_3 (*m/z* 619) (GlcNAc – UA – GlcNS), Z_5 (*m/z* 517) (GlcNS – UA – GlcNAc – UA – GlcNS), C_2 (*m/z* 496) (ΔUA2S – GlcNS) (Figure 4c and Table S-25). The presence of the second isomer ΔUA2**S** – GlcN**S** – UA – GlcN**S** – UA – GlcNAc (Table S-19 and Table S-25) was concluded due to the presence of Z_2 (*m/z* 378) (UA – GlcNAc), which was likely to be a contaminant from the adjacent peak eluting at 18 minutes. The structure eluting at 21 minutes (Figure 4d and Table S-20) was interpreted as ΔUA – GlcN**S**6**S** – UA – GlcN**S** – UA – GlcNAc. The important ions to deduce this structure was C_2 (*m/z* 496) (ΔUA – Glc6SNS) and Z_4 (*m/z* 795) (UA – GlcNS – UA – GlcNAc), confirming the positions of the O-sulfates, with other ions complementary to the sequence Z_2 (*m/z* 378) (UA – GlcNAc), Y_2 (*m/z* 396), Z_3 (*m/z* 619) (GlcNS – UA – GlcNAc), Y_4 (*m/z* 813) (UA – GlcNS – UA – GlcNAc). The structure eluting at 22 minutes shows that the sequence is ΔUA – GlcN**S** – UA – GlcNAc – UA –

GlcN**S**6**S** (Figure 4e and Table S-30). The C_2 (*m/z* 416) (ΔUA – GlcNS –), C_3 (*m/z* 592) (ΔUA – GlcNS – UA –), C_4 (*m/z* 795) (ΔUA – GlcNS – UA – GlcNAc –), B_3 (*m/z* 574) (ΔUA – GlcNS – UA), B_4 (*m/z* 777) (ΔUA – GlcNS – UA – GlcNAc), B_5 (*m/z* 476) (ΔUA – GlcNS – UA – GlcNAc – UA), Y_3 (*m/z* 717) (GlcNAc – UA – GlcNS6S) and Z_2 (*m/z* 496) (UA – GlcNS6S) ions support the final sequence.

Atypical structures identified using PGC LC-MS

Analysis of heparinase produced products has led to the general view that oligosaccharides with odd-numbers of monosaccharides are rare, since these enzymes only cleave between glucosamine and uronic acid[46]. SEC fractions derived from HS by heparinase depolymerisation will be expected to contain a variety of oligosaccharides consisting of varying lengths and sulfation, including these rare oligosaccharides[7]. An example of one of these structures was seen by PGC LC-MS of the fraction M (Figure S-1 and Figure 5a). PGC LC-MS of fraction M from SEC (Figure S-1) appeared to consist of an odd-number monosaccharide unit oligosaccharide (Figure 5a and Table S-4), with one of the structures present producing an $[M - H]^-$ precursor ion of *m/z* 592.1 (Figure 5a), which corresponds to a dp3 + $1SO_3$ group. The nearly full set of B, Y, C and Z ions from its MS/MS spectra confirmed that this structure has the sequence ΔUA – GlcN**S** – UA (Table S-38 and Figure 5b). This structure is consistent with trisaccharide structures observed previously as products from heparinase digests[7]. One possibility is that the dp3 fragment may have resulted from heparinase III digestion of the linker region, whilst a further and perhaps more likely possibility is that the manufacturing and chemical processing of porcine mucosal HS (as a by-product of heparin production) has resulted in smaller fragments, which can be heparinase III digested leaving some tri-saccharides products.

Oligosaccharide recovery from the PGC column.

Graphite has hydrophobic properties similar to that of a reverse phase material, and electronic properties that make it desirable for separation of sulfated oligosaccharides. The polarizable surface causes charge induced dipoles, and the oxidizing and reducing capabilities towards an analyte required an assessment of oligosaccharide yields from the PGC column. A purified heparin lyase digested dp6 + $8SO_3^{9-10}$ was used to assess PGC oligosaccharide recovery using UV detection (Figure S-8). The recovery yield of the dp6 + $8SO_3$ calculated from peak area was 96 % (Figure S-8).

Conclusions

Here we demonstrate that PGC LC-MS can be used for the effective analysis of HS oligosaccharides, with good separation, sensitivity and isomeric resolution. The data also demonstrated that hydrophobic and electronic properties of PGC play major roles in binding to, and dissociation of HS oligosaccharides from graphite. As the electronic modifier is constant throughout the gradient, this elution must be based on the compounds hydrophobic nature; the more sulfates on a small chain the more hydrophilic it will be, and the larger or higher dp causes an increase in hydrophobicity which delays its elution. Based on this notion it would be reasonable to suggest that if a cation such as an ammonium ion was masking a negative charge, then this would affect the retention of a structure to the graphite. This was consistent with the observation that ammonium adduction results in longer elution times. PGC LC-MS of these oligosaccharides has improved the separation and analysis of negatively charged saccharides by exploiting oligosaccharide ring units and negative charges.

PGC column separations can be challenging but also high resolving due to their ability to complex with analytes through hydrophobicity, anion exchange and changes in steric interactions, leading to unpredictable chromatography behaviour. In our studies we found that long equilibration times were required along with overnight storage in acetronitrile combined with an acid wash to prevent PGC oxidation and avoid inconsistent retention times. Retention times of the analyte can vary over time most likely due to column oxidation, utilising an acid wash improves the stability[29, 47]. Others have shown deterioration of the PGC columns over time, necessitating maintenance and regeneration procedures using tetrahydrofuran, acetone, trifluoroacetate, hydrochloric acid or sodium hydroxide[29, 47]. As long as the PGC column is maintained, high yields of oligosaccharides are achievable. Several articles have shown changes in retention time from PGC over hours, months and years[29, 47-48] and we observed small retention time variation. It has been speculated that the PGC layers may rearranged, and the redox state of the material may also change. Oxidation of PGC appears to increase the positive charge on the surface causing stronger retention of anions; reduction of PGC resulted in a decrease in anionic binding which is important in the binding of highly sulfated oligosaccharides. Others have shown that treatment of the column with H_2O_2 and sodium thiosulphate maintained the column in a more stable redox state[49]. It has also been shown that temperature, percentage of methanol / acetronitrile, concentration of carbonate ions, pH and acid washes can all effect the elution of structures from PGC. Since pH can also effect analyte elution lowering the pH to pH 7 from pH 7.7 with 10 mM ammonium bicarbonate would ensure that the peeling reaction of reducing disaccharides 3-O-sulfate residues does not occur[50]. We are currently exploring these options to improve and optimize PGC LCMS as a robust routine methodology for HS oligosaccharides, and further allow analysis on saccharides containing reducing terminal 3O-sulfate groups.

To improve routine structural analyses, PGC could be coupled orthogonally with other LC-MS methods currently available. Both SEC and RP-IP can be easily performed before or after the PGC step, as both methodologies use compatible buffer systems. HILIC would be compatible with an additional organic line increasing the percentage of acetonitrile, (if the method was placed after PGC), or water (if placed before PGC). Coupling methods to create multi-dimensional workflows could significantly improve oligosaccharide separation in the future over currently available methods.

Obtaining saccharides of sufficient purity and their definitive sequencing, are challenging problems within the HS field. This is due to the high proportion of isomeric structures present, and the direct effect of purity on the ability to sequence. HS saccharide sequencing is still a significant major challenge due to a large proportion of product ions being isomeric, especially as dp and sulfation increases. This is further complicated by potential sulfation loss. However, progress is being made, and the availability if fully defined HS structures prepared by chemical, enzymatic and chemoenzymatic syntheses is supporting furthering development in this area [40, 51-52]. As more pure oligosaccharides are sequenced it creates the possibility of database methodology through spectral matching and increased confidence in false discovery rate scoring. A method such as graphite LC-MS as demonstrated here, which provides high resolution separation of oligosaccharides and enhanced oligosaccharide purity, leads to simplified product ion spectra, improved confidence in sequence assignment, and provides a profiling tool for complex and isolated structures. Thus, these PGC-based methods should prove invaluable in understanding HS structure-activity relationships.

Acknowledgements

We acknowledge helpful comments from Prof David Fernig. Financial support for this research was provided by a PhD studentship to RM from the Medical Research Council (MRC) and Engineering and Physical Sciences Research (EPSRC) Council UK (UoL/MRC-EPSRC), a Senior Research Fellowship from the MRC to JET (G117/423), a Biotechnology and Biological Sciences Research Council project grant to JET (BB/I004343/1). NGK was supported by the Swedish Research Council (621-2013-5895), Kung Gustav V:s 80-års foundation, Petrus and Augusta Hedlund's foundation and the AFA insurance research fund.

Supporting Information Available: Figure S-1. SEC separation of heparinase I digested oligosaccharides produced from heparin. Figure S-2. LC-MS analysis of Arixtra. Figure S-3. Relative oligossaccharide abundance identified through LC-MS of SEC fraction A. Figure S-4. Relative oligossaccharide abundance identified through LC-MS of SEC fraction B. Figure S-5. Relative oligossaccharide abundance identified through LC-MS of SEC fraction C. Figure S-6. Relative oligossaccharide abundance identified through LC-MS of SEC fraction M. Figure S-7 SAX separation of SEC fraction A. Figure S-8. Recovery of dp6 + $8SO_3$ from the graphite column. Table S-1. LC-MS analysis of SEC fraction A. Table S-2. LC-MS analysis of SEC fraction B. Table S-3. LC-MS analysis of SEC fraction C. Table S-4. LC-MS analysis of SEC fraction M. Table S-5 and Table S-6, theoretical product ions of Peak F and G. Table S-7 to Table S-18, theoretical product ions of Peak H. Table S-19 to Table S-36, theoretical product ions of Peaks I, J, K, and L. Table S-37, summary of total theoretical product ions of Peaks I, J, K, and L. Table S-38, theoretical product ions of Peak O. Supporting information (45 pages). This material is available free of charge via the Internet at http://pubs.acs.org.

Figure 1. Workflow of oligosaccharide purification and PGC LC-MS analysis.

Figure 2. A high throughput method employing PGC LC-MS for analysis of oligosaccharides derived from PMHS. Each fraction was SEC separated (Figure S-1) and analysed using PGC LC-MS and MS/MS as a method for the analysis of several structures in a mixture. 2a) Separation of SEC fraction A using PGC LC-MS. 2b) Separation of SEC fraction B using PGC LC-MS. 2c) Separation of SEC fraction C using PGC LC-MS. The gradient in all cases was a 0-40% linear acetonitrile gradient with 10 mM ammonium bicarbonate.

Figure 3. Analysis of purified HS saccharides by PGC LC-MS. A SEC dp4 fraction (peak A, Figure S-1) was separated using SAX chromatography on a 0-2 M gradient over 150 mins (Figure S-2) and analysed through PGC LC-MS/MS. 3a) LC-MS of peak D and E. 3b) MS spectra of peaks F and G are shown on the bottom chromatogram with both peaks displaying an $[M - H]^-$ ion of *m/z* 795.2 and MS spectrum of peak H is shown in the top spectra displaying an $[M - 2H]^{2-}$ of *m/z* 477. 3c) MS/MS of the $[M - H]^-$ ion of *m/z* 795 from peak F corresponding to the structure ΔUA – GlcN**S** – UA – GlcNAc. 3d) MS/MS of the $[M - H]^-$ ion of *m/z* 795 from peak G corresponding to the structure ΔUA – GlcNAc – UA – GlcN**S**. 3e) MS/MS of the $[M - 2H]^{2-}$ ion of *m/z* 477 from peak H corresponding to the structure ΔUA – GlcN**S** – UA2**S** – GlcNAc6**S**. All fragments were assigned using Domon and Costello nomenclature using the Glycoworkbench software [38].

Figure 4. Extracted ion chromatogram of dp6 + 1Ac + 3SO_3 from Figure 2b. An EIC shows that PGC could separate isomeric structures isolated from SEC fraction B, which is a complex

mixture of dp6 and dp8 oligosaccharides. 4a) EIC of $[M - 2H]^{2-}$ ion of *m/z* 645.5 corresponding to a dp6 + 1Ac + $3SO_3$. 2b) MS/MS of peak I (18 mins) corresponding to the structure ΔUA2**S** - GlcN**S** - UA - GlcN**S** - UA - GlcNAc. 2c) MS/MS of peak J (20 mins) corresponding to the structure ΔUA2**S** - GlcN**S** - UA - GlcNAc - UA - GlcN**S**. 3d) MS/MS of peak K (21mins) corresponding to the structure ΔUA – GlcN**S6S** - UA - GlcN**S** - UA - GlcNAc. 2e) MS/MS of peak L (22 mins) corresponding to the structure ΔUA - GlcN**S** - UA - GlcNAc - UA – GlcN**S6S**.

Figure 5. Trisaccharide structures identified using LC-MS of PMHS digested products. Products of a heparinase III enzyme digest of PMHS were separated using SEC. Fraction M was separated and analysed using graphite LC-MS and MS/MS. 5a) Separation of fraction M using PGC LC-MS on a 0-40 % gradient using acetonitrile with 10 mM ammonium bicarbonate. Insert - MS of peak O, an ambiguous compound having an $[M - H]^-$ ion of *m/z* 592.1. 5c) MS/MS of the $[M - H]^-$ ion of *m/*z 592.1.

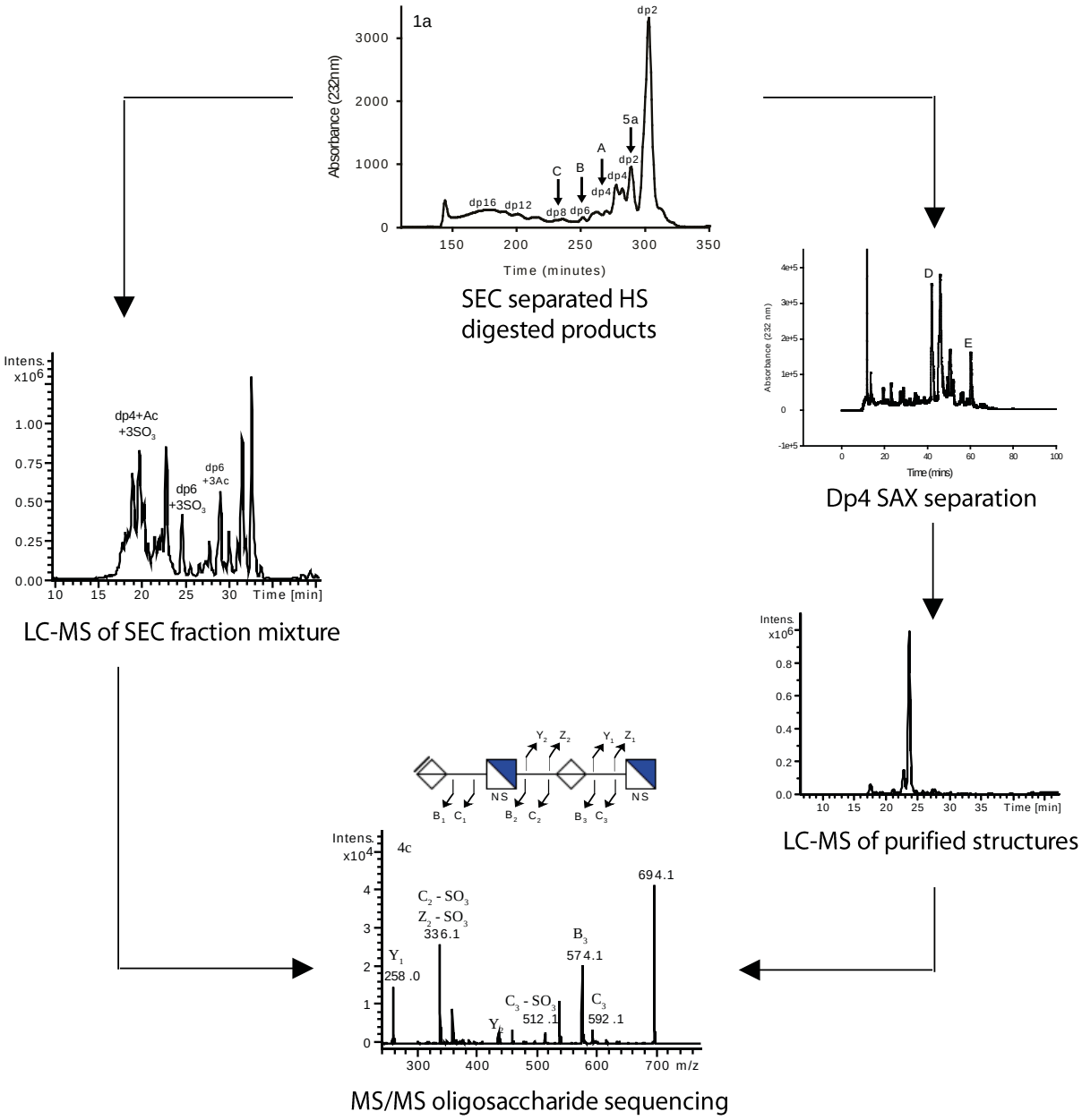

Figure 1. Workflow of oligosaccharide purification and PGC LC-MS analysis.

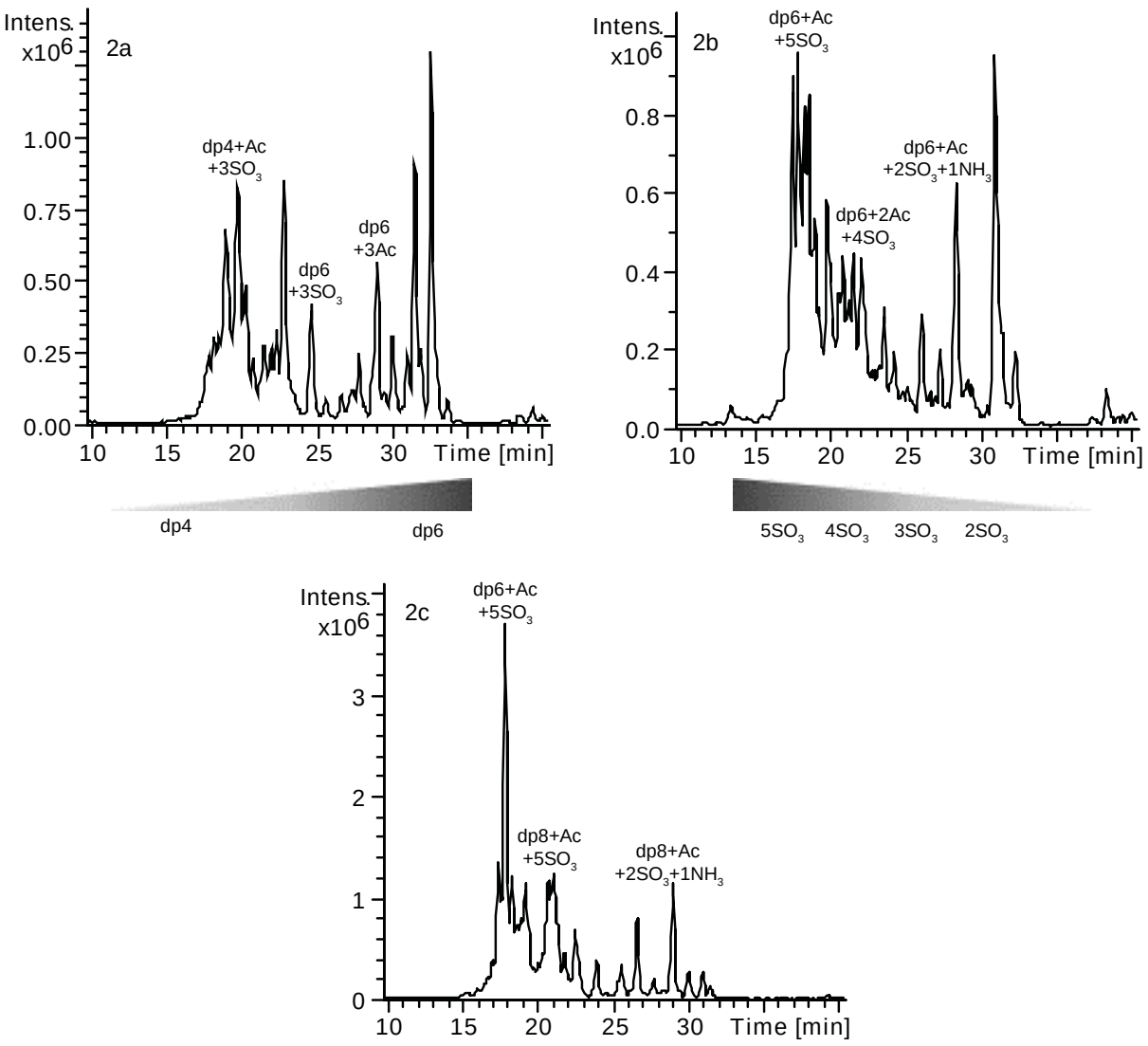

Figure 2. A high throughput method employing PGC LC-MS for analysis of oligosaccharides derived from PMHS.

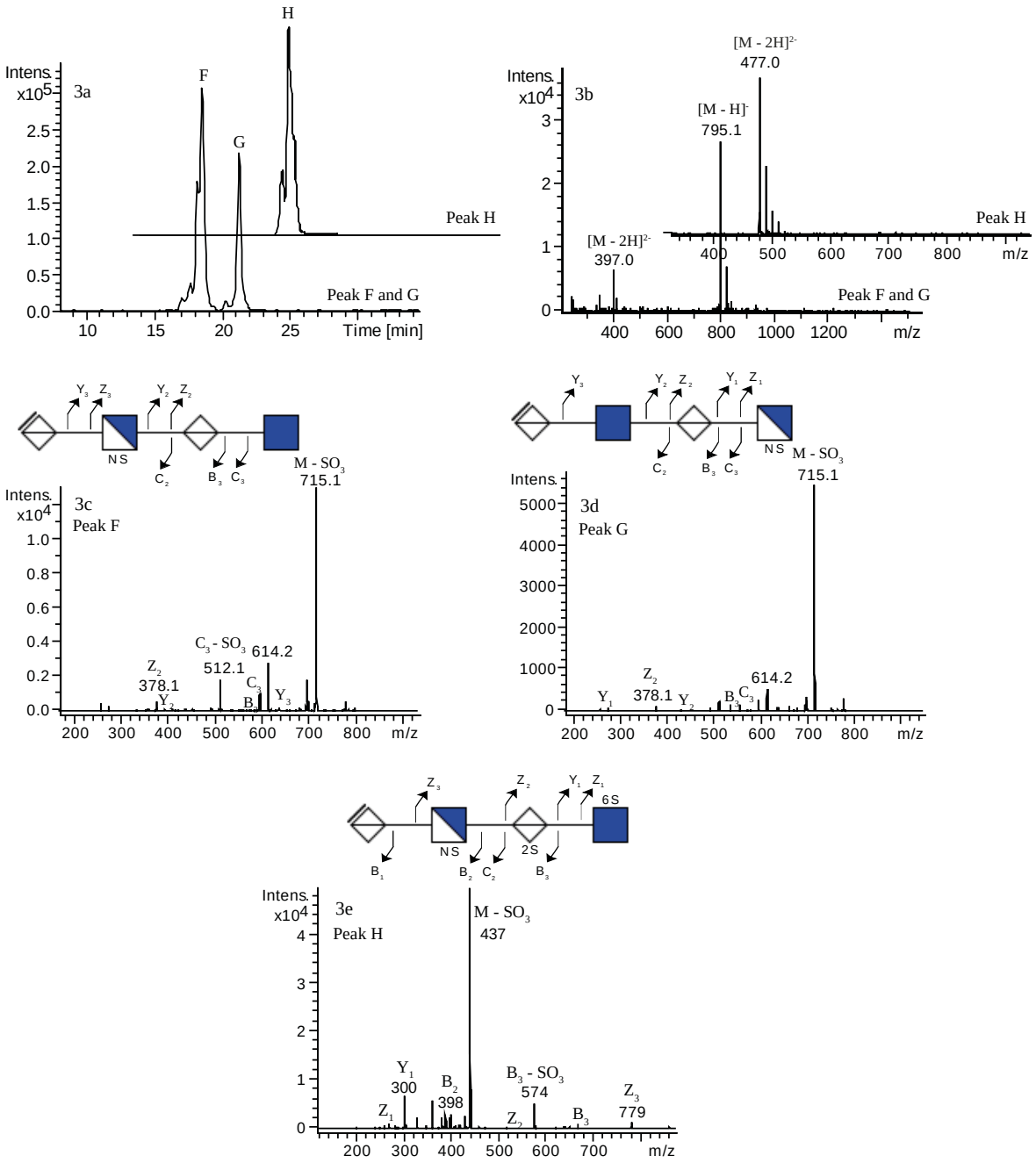

Figure 3. Analysis of purified HS saccharides by PGC LC-MS.

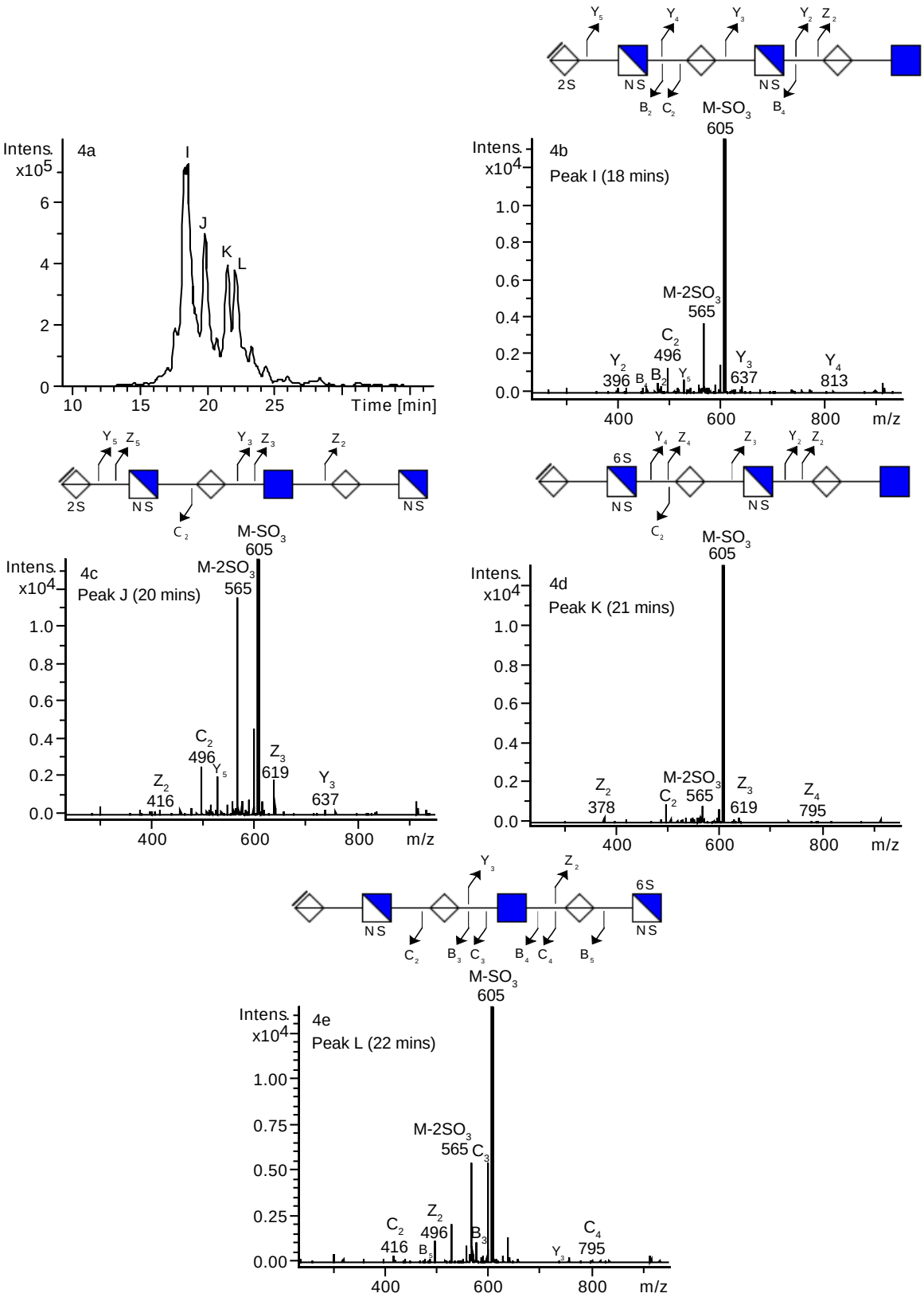
4a
Intens.
x10^5
I
J
K
L
Time [min]
4b
Peak I (18 mins)
Intens.
x10^4
M-SO3
605
M-2SO3
565
C2
496
Y2
396
Y3
637
Y4
813
m/z
4c
Peak J (20 mins)
Intens.
x10^4
M-SO3
605
M-2SO3
565
C2
496
Z3
619
Z2
416
Y3
637
m/z
4d
Peak K (21 mins)
Intens.
x10^4
M-SO3
605
Z2
378
M-2SO3
C2
565
Z3
619
Z4
795
m/z
4e
Peak L (22 mins)
Intens.
x10^4
M-SO3
605
M-2SO3
565
C3
Z2
496
C2
416
B3
C4
795
Y3
m/z

Figure 4. Extracted ion chromatogram of dp6 + 1Ac + 3SO_3 from figure 2b.

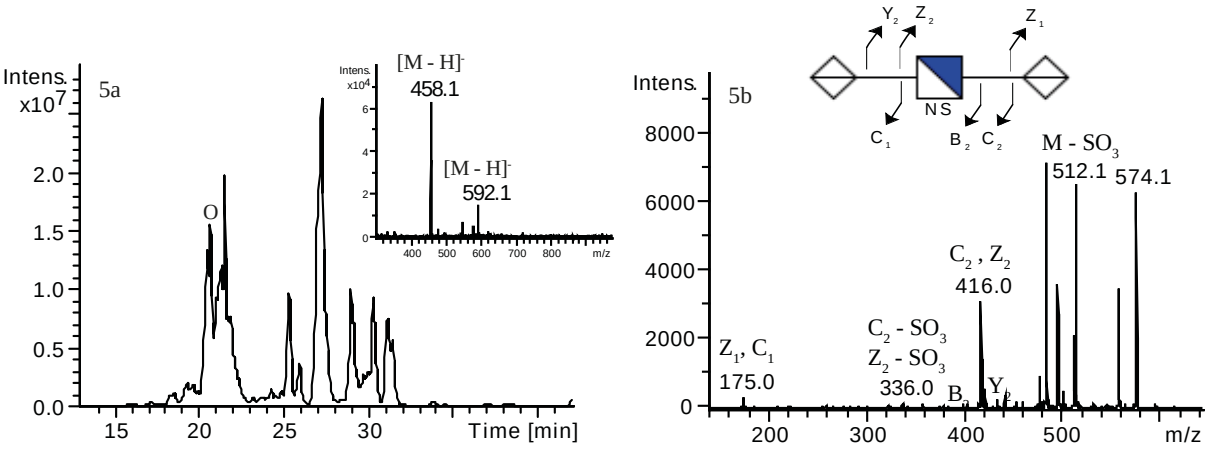

Figure 5. Trisaccharide structures identified using LC-MS of PMHS digested products.

References

1. Leymarie, N.; McComb, M. E.; Naimy, H.; Staples, G. O.; Zaia, J., *Int J Mass Spectrom* **2012,** *312*, 144-154.
2. Staples, G. O.; Shi, X.; Zaia, J., *PLoS One* **2011,** *6* (2), e16689.
3. Staples, G. O.; Shi, X.; Zaia, J., *J Biol Chem* **2010,** *285* (24), 18336-43.
4. Xu, D.; Esko, J. D., *Annu Rev Biochem* **2014,** *83*, 129-57.
5. Stewart, M. D.; Sanderson, R. D., *Matrix Biol* **2014,** *35*, 56-9.
6. Esko, J. D.; Selleck, S. B., *Annu Rev Biochem* **2002,** *71*, 435-71.
7. Ziegler, A.; Zaia, J., *J Chromatogr B Analyt Technol Biomed Life Sci* **2006,** *837* (1-2), 76-86.
8. Henriksen, J.; Ringborg, L. H.; Roepstorrf, P., *J Mass Spectrom* **2004,** *39* (11), 1305-12.
9. Miller, R. L.; Guimond, S. E.; Shivkumar, M.; Blocksidge, J.; Austin, J. A.; Leary, J. A.; Turnbull, J. E., *Anal Chem* **2016,** *88* (23), 11542-11550.
10. Miller, R. L.; Dykstra, A. B.; Wei, W.; Holsclaw, C.; Turnbull, J. E.; Leary, J. A., *Anal Chem* **2016,** *88* (23), 11551-11558.
11. Powell, A. K.; Ahmed, Y. A.; Yates, E. A.; Turnbull, J. E., *Nat Protoc* **2010,** *5* (5), 821-33.
12. Nice, E. C.; Capp, M.; O'Hare, M. J., *J Chromatogr* **1979,** *185*, 413-27.
13. Mahoney, W. C.; Hermodson, M. A., *J Biol Chem* **1980,** *255* (23), 11199-203.
14. Guo, Y. C.; Conrad, H. E., *Anal Biochem* **1988,** *168* (1), 54-62.
15. Thanawiroon, C.; Linhardt, R. J., *J Chromatogr A* **2003,** *1014* (1-2), 215-23.
16. Henriksen, J.; Roepstorff, P.; Ringborg, L. H., *Carbohydr Res* **2006,** *341* (3), 382-7.
17. Hoffmann, M.; Marx, K.; Reichl, U.; Wuhrer, M.; Rapp, E., *Mol Cell Proteomics* **2016,** *15* (2), 624-41.
18. Royle, L.; Roos, A.; Harvey, D. J.; Wormald, M. R.; van Gijlswijk-Janssen, D.; Redwan el, R. M.; Wilson, I. A.; Daha, M. R.; Dwek, R. A.; Rudd, P. M., *J Biol Chem* **2003,** *278* (22), 20140-53.
19. Akiyama, H.; Shidawara, S.; Mada, A.; Toyoda, H.; Toida, T.; Imanari, T., *J Chromatogr* **1992,** *579* (2), 203-7.
20. Saitoh, H.; Takagaki, K.; Majima, M.; Nakamura, T.; Matsuki, A.; Kasai, M.; Narita, H.; Endo, M., *J Biol Chem* **1995,** *270* (8), 3741-7.
21. Huang, Y.; Shi, X.; Yu, X.; Leymarie, N.; Staples, G. O.; Yin, H.; Killeen, K.; Zaia, J., *Anal Chem* **2011,** *83* (21), 8222-9.
22. Hitchcock, A. M.; Yates, K. E.; Costello, C. E.; Zaia, J., *Proteomics* **2008,** *8* (7), 1384-97.
23. Staples, G. O.; Bowman, M. J.; Costello, C. E.; Hitchcock, A. M.; Lau, J. M.; Leymarie, N.; Miller, C.; Naimy, H.; Shi, X.; Zaia, J., *Proteomics* **2009,** *9* (3), 686-95.
24. Karlsson, N. G.; Schulz, B. L.; Packer, N. H., *J Am Soc Mass Spectrom* **2004,** *15* (5), 659-72.
25. Karlsson, N. G.; Wilson, N. L.; Wirth, H. J.; Dawes, P.; Joshi, H.; Packer, N. H., *Rapid Commun Mass Spectrom* **2004,** *18* (19), 2282-92.
26. Kawasaki, N.; Haishima, Y.; Ohta, M.; Itoh, S.; Hyuga, M.; Hyuga, S.; Hayakawa, T., *Glycobiology* **2001,** *11* (12), 1043-9.
27. Koizumi, K., *J Chromatogr A* **1996,** *720* (1-2), 119-26.

28. Reepmeyer, J. C.; Brower, J. F.; Ye, H., *J Chromatogr A* **2005,** *1083* (1-2), 42-51.
29. Pabst, M.; Altmann, F., *Anal Chem* **2008,** *80* (19), 7534-42.
30. Karlsson, N. G.; Schulz, B. L.; Packer, N. H.; Whitelock, J. M., *J Chromatogr B Analyt Technol Biomed Life Sci* **2005,** *824* (1-2), 139-47.
31. Costello, C. E.; Contado-Miller, J. M.; Cipollo, J. F., *J Am Soc Mass Spectrom* **2007,** *18* (10), 1799-812.
32. Estrella, R. P.; Whitelock, J. M.; Packer, N. H.; Karlsson, N. G., *Anal Chem* **2007,** *79* (10), 3597-606.
33. Saad, O. M.; Leary, J. A., *Anal Chem* **2003,** *75* (13), 2985-95.
34. Wei, W.; Ninonuevo, M. R.; Sharma, A.; Danan-Leon, L. M.; Leary, J. A., *Anal Chem* **2011,** *83* (10), 3703-8.
35. Wei, W.; Miller, R. L.; Leary, J. A., *Anal Chem* **2013,** *85* (12), 5917-23.
36. Shao, C.; Shi, X.; Phillips, J. J.; Zaia, J., *Anal Chem* **2013,** *85* (22), 10984-91.
37. Hitchcock, A. M.; Yates, K. E.; Shortkroff, S.; Costello, C. E.; Zaia, J., *Glycobiology* **2007,** *17* (1), 25-35.
38. Ceroni, A.; Maass, K.; Geyer, H.; Geyer, R.; Dell, A.; Haslam, S. M., *J Proteome Res* **2008,** *7* (4), 1650-9.
39. Domon, B.; Costello, C. E., *Glycoconjugate Journal* **1988,** *5* (4), 397-409.
40. Miller, R. L.; Leary, J. A.; Wei, W.; Schworer, R.; Zubkova, O. V.; Tyler, P. C.; Turnbull, J. E., *Eur J Mass Spectrom (Chichester)* **2015,** *21* (3), 245-54.
41. Wolff, J. J.; Leach, F. E., 3rd; Laremore, T. N.; Kaplan, D. A.; Easterling, M. L.; Linhardt, R. J.; Amster, I. J., *Anal Chem* **2010,** *82* (9), 3460-6.
42. Wolff, J. J.; Amster, I. J.; Chi, L.; Linhardt, R. J., *J Am Soc Mass Spectrom* **2007,** *18* (2), 234-44.
43. Wolff, J. J.; Chi, L.; Linhardt, R. J.; Amster, I. J., *Anal Chem* **2007,** *79* (5), 2015-22.
44. Shi, X.; Huang, Y.; Mao, Y.; Naimy, H.; Zaia, J., *J Am Soc Mass Spectrom* **2012,** *23* (9), 1498-511.
45. Leary, J. A.; Miller, R. L.; Wei, W.; Schworer, R.; Zubkova, O. V.; Tyler, P. C.; Turnbull, J. E., *Eur J Mass Spectrom (Chichester, Eng)* **2015,** *21* (3), 245-54.
46. Linhardt, R. J.; Turnbull, J. E.; Wang, H. M.; Loganathan, D.; Gallagher, J. T., *Biochemistry* **1990,** *29* (10), 2611-7.
47. Pabst, M.; Grass, J.; Fischl, R.; Leonard, R.; Jin, C.; Hinterkorner, G.; Borth, N.; Altmann, F., *Anal Chem* **2010,** *82* (23), 9782-8.
48. Bapiro, T. E.; Richards, F. M.; Jodrell, D. I., *Anal Chem* **2016,** *88* (12), 6190-4.
49. Jansen, R. S.; Rosing, H.; Schellens, J. H.; Beijnen, J. H., *Rapid Commun Mass Spectrom* **2009,** *23* (19), 3040-50.
50. Huang, Y.; Mao, Y.; Zong, C.; Lin, C.; Boons, G. J.; Zaia, J., *Anal Chem* **2015,** *87* (1), 592-600.
51. Huang, R.; Zong, C.; Venot, A.; Chiu, Y.; Zhou, D.; Boons, G. J.; Sharp, J. S., *Anal Chem* **2016,** *88* (10), 5299-307.
52. Huang, R.; Liu, J.; Sharp, J. S., *Anal Chem* **2013,** *85* (12), 5787-95.

Supporting Information

Versatile Separation and Analysis of Heparan Sulfate Oligosaccharides using Graphitised Carbon Liquid Chromatography and Electrospray Mass Spectrometry

Rebecca L. Miller[1,3], Scott E. Guimond[1], Mark Prescott[1], Jeremy E. Turnbull[1]*.and Niclas Karlsson[2]*.

[1]Centre for Glycobiology, Department of Biochemistry, Institute of Integrative Biology, University of Liverpool, Crown Street, Liverpool, L69 7ZB, England, UK;

[2]The Sahlgrenska Academy, Institute of Biomedicine, University of Gothenburg, Box 400 40530 Göteborg, Sweden.

[3]Univeristy Of Oxford, Oncology Department, Old Road Campus Research Building, Oxford, OX3 7DQ

*Joint senior authors

Authors email address: rebecca.miller@oncology.ox.ac.uk

Corresponding Authors;

Rebecca L. Miller

Email address: rebecca.miller@oncology.ox.ac.uk

Prof. Jeremy Turnbull

Email address: j.turnbull@liverpool.ac.uk

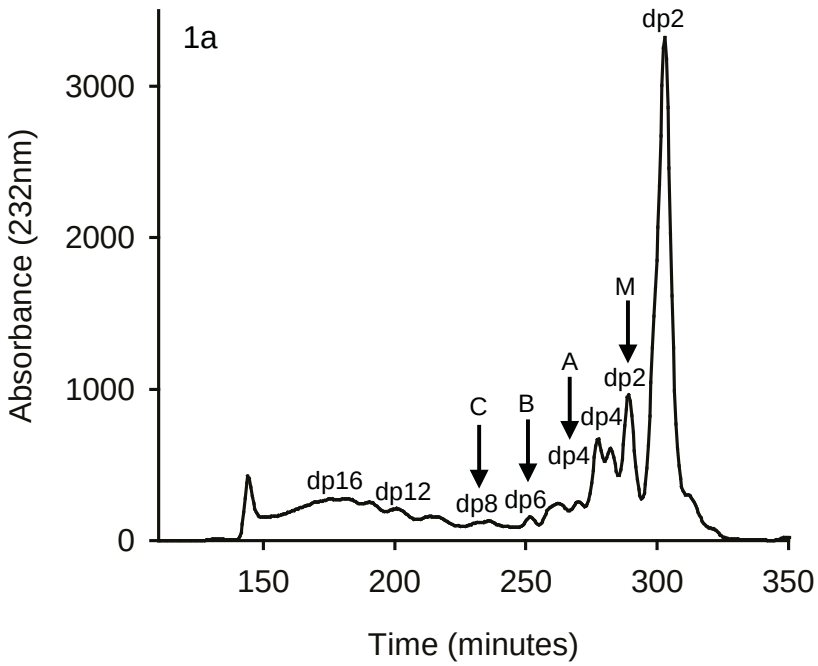

Figure S-1. Products of a heparinase III enzyme digest of PMHS were separated using SEC and selected fractions as shown collected for further experiments.

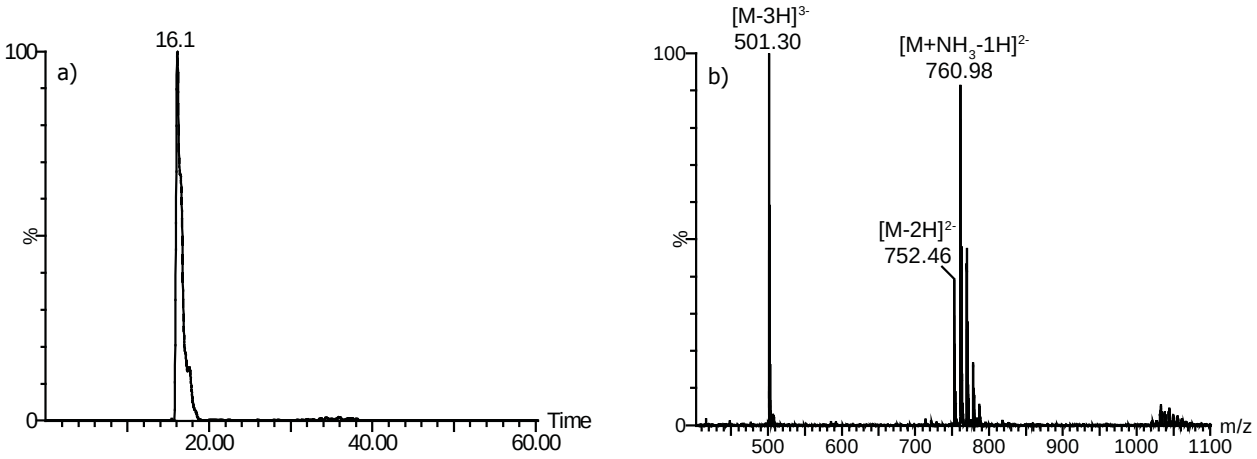

Figure S-2. PGC LC-MS analysis of Arixtra. a) PGC LC-MS of Arixtra on a 0-40 % gradient resulted in the elution of Arixtra at 16.1 minutes from the EIC. b) MS of Arixtra at 16.1 minutes.

Table S-1. PGC LC-MS analysis of SEC fraction A obtained from heparinase III digested PMHS. Compounds were identified based on MS and MS/MS spectra and placed in elution order. The oligosaccharide style established by Zaia et al was used in oligosaccharide characterization, as follows; [ΔHexA, HexA, GlcN, SO_3, Ac, Na, NH_3].

Time (mins)	*m/z*	[ΔHexA, HexA, GlcN, SO_3, Ac, Na, NH_3]	Composition
17-18	955 $[M-H]^-$, 477.0 $[M-2H]^{2-}$	1, 1, 2, 3, 1, 0, 0	dp4 +Ac + $3SO_3$
	1372.2 $[M-H]^-$, 685.6 $[M-2H]^{2-}$	1, 2, 3, 4, 1, 0, 0	dp6 + Ac + $4SO_3$
18-19	1292 $[M-H]^-$, 645.6 $[M-2H]^{2-}$	1, 2, 3, 3, 1, 0, 0	dp6 + Ac + $3SO_3$
	955 $[M-H]^-$, 477.0 $[M-2H]^{2-}$	1, 1, 2, 3, 1, 0, 0	dp4 +Ac + $3SO_3$
	1035 $[M-H]^-$, 517.0 $[M-2H]^{2-}$	1, 1, 2, 4, 1, 0, 0	dp4 + Ac + $4SO_3$
	1372.2 $[M-H]^-$, 685.6 $[M-2H]^{2-}$	1, 2, 3, 4, 1, 0, 0	dp6 + Ac + $4SO_3$
19-20	955 $[M-H]^-$, 477.0 $[M-2H]^2$	1, 1, 2, 3, 1, 0, 0	dp4 +Ac + $3SO_3$
	993 $[M-H]^-$, 496.0 $[M-2H]^{2-}$	1, 1, 2, 4, 0, 0, 0	dp4 + $4SO_3$
	1212.2 $[M-H]^-$ 605.6 $[M-2H]^{2-}$	1, 2, 3, 2, 1, 0, 0	dp6 + Ac + $2SO_3$
	1292.2 $[M-H]^-$, 645.6 $[M-2H]^{2-}$	1, 2, 3, 3, 1, 0, 0	dp6 + Ac + $3SO_3$
	1372.2 $[M-H]^-$, 685.6 $[M-2H]^{2-}$	1, 2, 3, 4, 1, 0, 0	dp6 + Ac + $4SO_3$
20-21	955 $[M-H]^-$, 477.0 $[M-2H]^2$	1, 1, 2, 3, 1, 0, 0	dp4 +Ac + $3SO_3$
	1212.2 $[M-H]^-$, 605.6 $[M-2H]^{2-}$	1, 2, 3, 2, 1, 0, 0	dp6 + Ac + $2SO_3$
	1292.2 $[M-H]^-$, 645.6 $[M-2H]^{2-}$	1, 2, 3, 3, 1, 0, 0	dp6 + Ac + $3SO_3$
	1330.2 $[M-H]^-$, 664.6 $[M-2H]^{2-}$	1, 2, 3, 4, 0, 0, 0	dp6 + $4SO_3$
21-22	1170.2 $[M-H]^-$, 584.6 $[M-2H]^{2-}$	1, 2, 3, 2, 0, 0, 0	dp6 + $2SO_3$
	1212.2 $[M-H]^-$, 605.6 $[M-2H]^{2-}$	1, 2, 3, 2, 1, 0, 0	dp6 + Ac + $2SO_3$
	1250.2 $[M-H]^-$, 624.6 $[M-2H]^{2-}$	1, 2, 3, 3, 0, 0, 0	dp6 + $3SO_3$
	1292.2 $[M-H]^-$, 645.6 $[M-2H]^{2-}$	1, 2, 3, 3, 1, 0, 0	dp6 + Ac + $3SO_3$
	1330.2 $[M-H]^-$, 664.6 $[M-2H]^{2-}$	1, 2, 3, 4, 0, 0, 0	dp6 + $4SO_3$
22-23	1250.2 $[M-H]^-$, 624.6 $[M-2H]^{2-}$	1, 2, 3, 3, 0, 0, 0	dp6 + $3SO_3$
	1212.2 $[M-H]^-$, 645.6 $[M-2H]^{2-}$	1, 2, 3, 2, 1, 0, 0	dp6 + Ac + $2SO_3$
	1250.2 $[M-H]^-$, 624.6 $[M-2H]^{2-}$	1, 2, 3, 3, 0, 0, 0	dp6 + $3SO_3$
	1334.2 $[M-H]^-$, 666.6 $[M-2H]^{2-}$	1, 2, 3, 3, 2, 0, 0	dp6 + 2Ac + $3SO_3$
23-24	1250.2 $[M-H]^-$, 624.6 $[M-2H]^{2-}$	1, 2, 3, 3, 0, 0, 0	dp6 + $3SO_3$
	1132.2 $[M-H]^-$, 565.6 $[M-2H]^{2-}$	1, 2, 3, 1, 1, 0, 0	dp6 + Ac + $1SO_3$
	1170.2 $[M-H]^-$, 584.6 $[M-2H]^{2-}$	1, 2, 3, 2, 0, 0, 0	dp6 + $2SO_3$
	1212.2 $[M-H]^-$, 605.6 $[M-2H]^{2-}$	1, 2, 3, 2, 1, 0, 0	dp6 + Ac + $2SO_3$
	1234.2 $[M-H]^-$, 616.6 $[M-2H]^{2-}$	1, 2, 3, 2, 1, 1, 0	dp6 + Ac + $2SO_3$ + 1Na
	1250.2 $[M-H]^-$, 624.6 $[M-2H]^{2-}$	1, 2, 3, 3, 0, 0, 0	dp6 + $3SO_3$
	1292.2 $[M-H]^-$, 645.6 $[M-2H]^{2-}$	1, 2, 3, 3, 1, 0, 0	dp6 + Ac + $3SO_3$
	1330.2 $[M-H]^-$, 664.6 $[M-2H]^{2-}$	1, 2, 3, 4, 0, 0, 0	dp6 + $4SO_3$
	1356.2 $[M-H]^-$, 677.2 $[M-2H]^{2-}$	1, 2, 3, 3, 2, 1, 0	dp6 + 2Ac + $3SO_3$ + 1Na
24-25	1132.2 $[M-H]^-$, 565.6 $[M-2H]^{2-}$	1, 2, 3, 1, 1, 0, 0	dp6 + Ac + $1SO_3$
	1170.2 $[M-H]^-$, 584.6 $[M-2H]^{2-}$	1, 2, 3, 2, 0, 0, 0	dp6 + $2SO_3$
	1212.2 $[M-H]^-$, 605.6 $[M-2H]^{2-}$	1, 2, 3, 2, 1, 0, 0	dp6 + Ac + $2SO_3$
	1250.2 $[M-H]^-$, 624.6 $[M-2H]^{2-}$	1, 2, 3, 3, 0, 0, 0	dp6 + $3SO_3$

	1334.2 $[M-H]^-$, 666.6 $[M-2H]^{2-}$	1, 2, 3, 3, 2, 0, 0	dp6 + 2Ac + $3SO_3$
	1356.2 $[M-H]^-$, 677.2 $[M-2H]^{2-}$	1, 2, 3, 3, 2, 1, 0	dp6 + 2Ac + $3SO_3$ + 1Na
25-26	1019 $[M-H]^-$, 509.0 $[M-2H]^{2-}$	1, 1, 2, 3, 2, 1, 0	dp4 + 2Ac + $3SO_3$ + 1Na
	1116.2 $[M-H]^-$, 557.6 $[M-2H]^{2-}$	1, 2, 3, 0, 2, 1, 0	dp6 + 2Ac + 1Na
	1212.2 $[M-H]^-$, 605.6 $[M-2H]^{2-}$	1, 2, 3, 2, 1, 0, 0	dp6 + Ac + $2SO_3$
	1276.2 $[M-H]^-$, 637.6 $[M-2H]^{2-}$	1, 2, 3, 2, 2, 1, 0	dp6 + 2Ac + $2SO_3$ + 1Na
	1356.2 $[M-H]^-$, 677.2 $[M-2H]^{2-}$	1, 2, 3, 3, 2, 1, 0	dp6 + 2Ac + $3SO_3$ + 1Na
26-27	1356.2 $[M-H]^-$, 677.2 $[M-2H]^{2-}$	1, 2, 3, 3, 2, 1, 0	dp6 + 2Ac + $3SO_3$ + 1Na
27-28	1136.2 $[M-H]^-$, 578.6 $[M-2H]^{2-}$	1, 2, 3, 0, 3, 1, 0	dp6 + 3Ac + 1Na
	1170.2 $[M-H]^-$, 584.6 $[M-2H]^{2-}$	1, 2, 3, 2, 0, 0, 0	dp6 + $2SO_3$
	1276.2 $[M-H]^-$, 637.6 $[M-2H]^{2-}$	1, 2, 3, 2, 2, 1, 0	dp6 + 2Ac + $2SO_3$ + 1Na
	1294 $[M-H]^-$, 646.5 $[M-2H]^{2-}$	1, 2, 3, 3, 0, 2, 0	dp6 + $3SO_3$ + 2Na
	1389 $[M-H]^-$, 694.2 $[M-2H]^{2-}$	1, 3, 4, 0, 1, 0, 0	dp8 + Ac

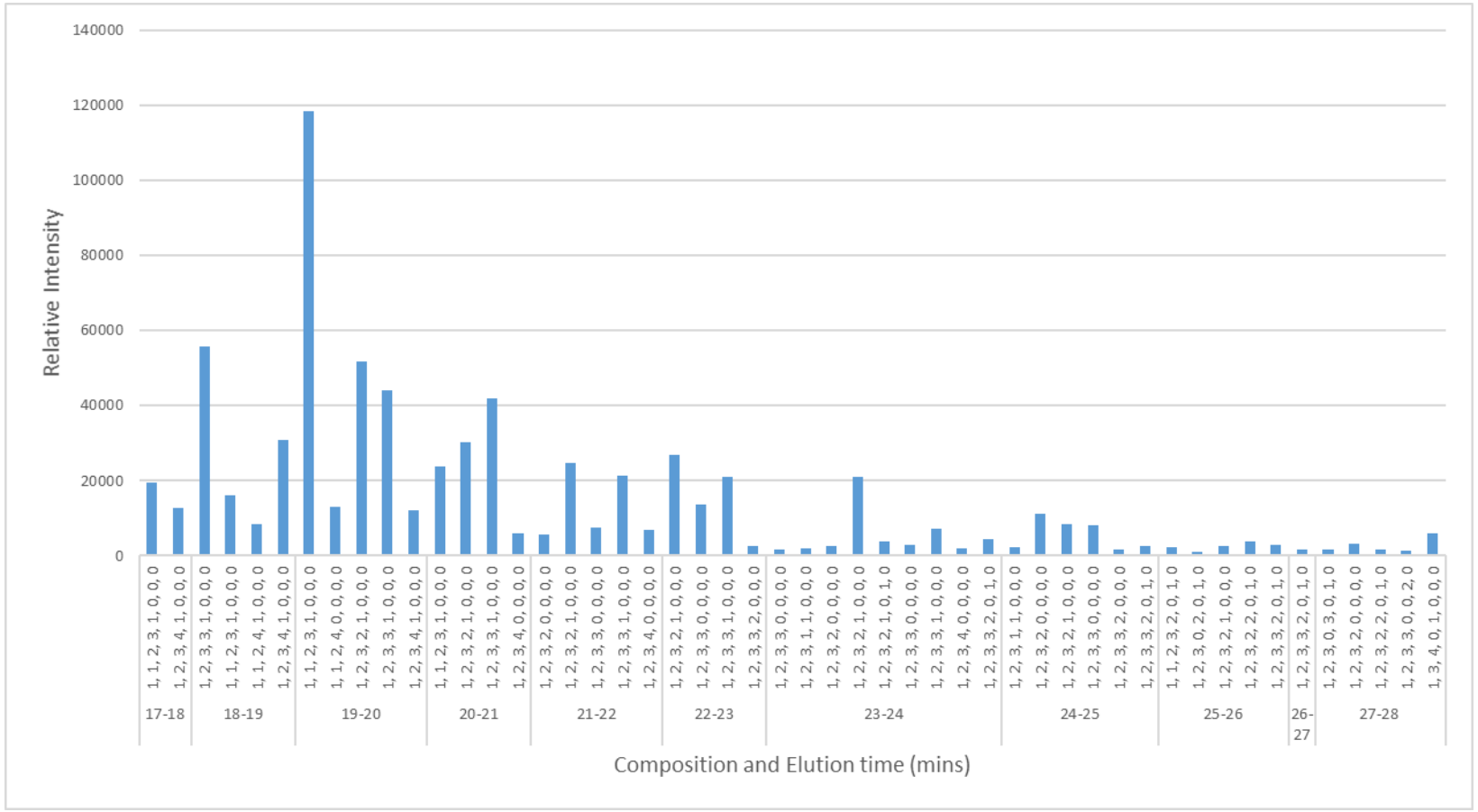

Figure S-3. Relative abundance of each oligosaccharide identified through PGC-LC-MS of SEC fraction A obtained from heparinase III digested PMHS. Compounds were identified based on MS and MS/MS spectra and placed in elution order. The oligosaccharide style is as described in Table S-1.

Table S-2. PGC LC-MS analysis of SEC fraction B obtained from heparinase III digested PMHS. Compounds were identified based on MS and MS/MS spectra and placed in elution order. The oligosaccharide style is as described in Table S-1.

Time (mins)	*m/z*	[ΔHexA, HexA, GlcN, SO_3, Ac, Na, NH_3]	Composition
17-18	1372.2 $[M-H]^-$, 685.6 $[M-2H]^{2-}$	1, 2, 3, 4, 1, 0, 0	dp6 + Ac + $4SO_3$
	1452 $[M-H]^-$, 725.5 $[M-2H]^{2-}$	1, 2, 3, 5, 1, 0, 0	dp6 + Ac + $5SO_3$
18-19	1292.2 $[M-H]^-$, 645.6 $[M-2H]^{2-}$	1, 2, 3, 3, 1, 0, 0	dp6 + Ac + $3SO_3$
	1372.2 $[M-H]^-$, 685.6 $[M-2H]^{2-}$	1, 2, 3, 4, 1, 0, 0	dp6 + Ac + $4SO_3$
	1452 $[M-H]^-$, 725.5 $[M-2H]^{2-}$	1, 2, 3, 5, 1, 0, 0	dp6 + Ac + $5SO_3$
19-20	1212.2 $[M-H]^-$, 605.6 $[M-2H]^{2-}$	1, 2, 3, 2, 1, 0, 0	dp6 + Ac + $2SO_3$
	1292.2 $[M-H]^-$, 645.6 $[M-2H]^{2-}$	1, 2, 3, 3, 1, 0, 0	dp6 + Ac + $3SO_3$
	1372.2 $[M-H]^-$, 685.6 $[M-2H]^{2-}$	1, 2, 3, 4, 1, 0, 0	dp6 + Ac + $4SO_3$
	1410 $[M-H]^-$, 704.5 $[M-2H]^{2-}$	1, 2, 3, 5, 0, 0, 0	dp6 + $5SO_3$
	1452 $[M-H]^-$, 725.5 $[M-2H]^{2-}$	1, 2, 3, 5, 1, 0, 0	dp6 + Ac + $5SO_3$
20-21	1212.2 $[M-H]^-$, 605.6 $[M-2H]^{2-}$	1, 2, 3, 2, 1, 0, 0	dp6 + Ac + $2SO_3$
	1292.2 $[M-H]^-$, 645.6 $[M-2H]^{2-}$	1, 2, 3, 3, 1, 0, 0	dp6 + Ac + $3SO_3$
	1372.2 $[M-H]^-$, 685.6 $[M-2H]^{2-}$	1, 2, 3, 4, 1, 0, 0	dp6 + Ac + $4SO_3$
	1410 $[M-H]^-$, 704.5 $[M-2H]^{2-}$	1, 2, 3, 5, 0, 0, 0	dp6 + $5SO_3$
21-22	1212.2 $[M-H]^-$, 605.6 $[M-2H]^{2-}$	1, 2, 3, 2, 1, 0, 0	dp6 + Ac + $2SO_3$
	1250.2 $[M-H]^-$, 624.6 $[M-2H]^{2-}$	1, 2, 3, 3, 0, 0, 0	dp6 + $3SO_3$
	1292.2 $[M-H]^-$, 645.6 $[M-2H]^{2-}$	1, 2, 3, 3, 1, 0, 0	dp6 + Ac + $3SO_3$
	1334.2 $[M-H]^-$, 666.6 $[M-2H]^{2-}$	1, 2, 3, 3, 2, 0, 0	dp6 + 2Ac + $3SO_3$
	1356 $[M-H]^-$, 677.5 $[M-2H]^{2-}$	1, 2, 3, 3, 2, 1, 0	dp6 + 2Ac + $3SO_3$ + 1Na
	1372.2 $[M-H]^-$, 685.6 $[M-2H]^{2-}$	1, 2, 3, 4, 1, 0, 0	dp6 + Ac + $4SO_3$
	1414.2 $[M-H]^-$, 706.6 $[M-2H]^{2-}$	1, 2, 3, 4, 2, 0, 0	dp6 + 2Ac + $4SO_3$
	1436 $[M-H]^-$, 717.5 $[M-2H]^{2-}$	1, 2, 3, 4, 2, 1, 0	dp6 + 2Ac + $4SO_3$ + 1Na
	1549.4 $[M-H]^-$, 774.2 $[M-2H]^{2-}$	1, 3, 4, 2, 1, 0, 0	dp8 + Ac + $2SO_3$
22-23	1212.2 $[M-H]^-$, 605.6 $[M-2H]^{2-}$	1, 2, 3, 2, 1, 0, 0	dp6 + Ac + $2SO_3$
	1292.2 $[M-H]^-$, 645.6 $[M-2H]^{2-}$	1, 2, 3, 3, 1, 0, 0	dp6 + Ac + $3SO_3$
	1372.2 $[M-H]^-$, 685.6 $[M-2H]^{2-}$	1, 2, 3, 4, 1, 0, 0	dp6 + Ac + $4SO_3$
	1549.4 $[M-H]^-$, 774.2 $[M-2H]^{2-}$	1, 3, 4, 2, 1, 0, 0	dp8 + Ac + $2SO_3$
23-24	1212. $[M-H]^-$, 605.6 $[M-2H]^{2-}$	1, 2, 3, 2, 1, 0, 0	dp6 + Ac + $2SO_3$
	1232 $[M-H]^-$, 615.5 $[M-2H]^{2-}$	1, 2, 3, 1, 3, 0, 1	dp6 + 3Ac + $1SO_3$ + $1NH_3$
	1254.2 $[M-H]^-$, 626.6 $[M-2H]^{2-}$	1, 2, 3, 2, 2, 0, 0	dp6 + 2Ac + $2SO_3$
	1292.2 $[M-H]^-$, 645.6 $[M-2H]^{2-}$	1, 2, 3, 3, 1, 0, 0	dp6 + Ac + $3SO_3$
	1330.2 $[M-H]^-$, 664.6 $[M-2H]^{2-}$	1, 1, 2, 4, 0, 0, 0	dp4 + $4SO_3$
	1356 $[M-H]^-$, 677.5 $[M-2H]^{2-}$	1, 2, 3, 3, 2, 1, 0	dp6 + 2Ac + $3SO_3$ + 1Na
	1372.2 $[M-H]^-$, 685.6 $[M-2H]^{2-}$	1, 2, 3, 4, 1, 0, 0	dp6 + Ac + $4SO_3$
	1469 $[M-H]^-$, 734.2 $[M-2H]^{2-}$	1, 3, 4, 1, 1, 0, 0	dp8 + Ac + $1SO_3$
24-25	1212.2 $[M-H]^-$, 605.6 $[M-2H]^{2-}$	1, 2, 3, 2, 1, 0, 0	dp6 + Ac + $2SO_3$
	1250.2 $[M-H]^-$, 624.6 $[M-2H]^{2-}$	1, 2, 3, 3, 0, 0, 0	dp6 + $3SO_3$

	1276 $[M-H]^-$, 637.5 $[M-2H]^{2-}$	1, 2, 3, 2, 2, 1, 0	dp6 + 2Ac + $2SO_3$ + 1Na
	1292.2 $[M-H]^-$, 645.6 $[M-2H]^{2-}$	1, 2, 3, 3, 1, 0, 0	dp6 + Ac + $3SO_3$
	1334.2 $[M-H]^-$, 666.6 $[M-2H]^{2-}$	1, 2, 3, 3, 2, 0, 0	dp6 + 2Ac + $3SO_3$
	1356 $[M-H]^-$, 677.5 $[M-2H]^{2-}$	1, 2, 3, 3, 2, 1, 0	dp6 + 2Ac + $3SO_3$ + 1Na
	1392.2 $[M-H]^-$, 695.6 $[M-2H]^{2-}$	1, 2, 3, 3, 3, 0, 1	dp6 + 3Ac + $3SO_3$ + $1NH_3$
	1436 $[M-H]^-$, 717.5 $[M-2H]^{2-}$	1, 2, 3, 4, 2, 1, 0	dp6 + 2Ac + $4SO_3$ + 1Na
	1469 $[M-H]^-$, 734.2 $[M-2H]^{2-}$	1, 3, 4, 1, 1, 0, 0	dp8 + Ac + $1SO_3$
	1549.4 $[M-H]^-$, 774.2 $[M-2H]^{2-}$	1, 3, 4, 2, 1, 0, 0	dp8 + Ac + $2SO_3$
25-26	1212.2 $[M-H]^-$, 605.6 $[M-2H]^{2-}$	1, 2, 3, 2, 1, 0, 0	dp6 + Ac + $2SO_3$
	1276 $[M-H]^-$, 637.5 $[M-2H]^{2-}$	1, 2, 3, 2, 2, 1, 0	dp6 + 2Ac + $2SO_3$ + 1Na
	1292.2 $[M-H]^-$, 645.6 $[M-2H]^{2-}$	1, 2, 3, 3, 1, 0, 0	dp6 + Ac + $3SO_3$
	1334.2 $[M-H]^-$, 666.6 $[M-2H]^{2-}$	1, 2, 3, 3, 2, 0, 0	dp6 + 2Ac + $3SO_3$
	1356 $[M-H]^-$, 677.5 $[M-2H]^{2-}$	1, 2, 3, 3, 2, 1, 0	dp6 + 2Ac + $3SO_3$ + 1Na
	1363.4 $[M-H]^-$, 681.2 $[M-2H]^{2-}$	1, 3, 4, 0, 0, 0, 1	dp8 + $1NH_3$
	1405.4 $[M-H]^-$, 703.2 $[M-2H]^{2-}$	1, 3, 4, 0, 1, 0, 1	dp8 + Ac + $1NH_3$
	1427.4 $[M-H]^-$, 713.2 $[M-2H]^{2-}$	1, 3, 4, 1, 0, 0, 0	dp8 + $1SO_3$
	1469 $[M-H]^-$, 734.2 $[M-2H]^{2-}$	1, 3, 4, 1, 1, 0, 0	dp8 + Ac + $1SO_3$
	1489 $[M-H]^-$, 744.1 $[M-2H]^{2-}$	1, 3, 4, 0, 3, 0, 1	dp8 + 3Ac + $1NH_3$
26-27	1212.2 $[M-H]^-$, 605.6 $[M-2H]^{2-}$	1, 2, 3, 2, 1, 0, 0	dp6 + Ac + $2SO_3$
	1250.2 $[M-H]^-$, 624.6 $[M-2H]^{2-}$	1, 2, 3, 3, 0, 0, 0	dp6 + $3SO_3$
	1276 $[M-H]^-$, 637.5 $[M-2H]^{2-}$	1, 2, 3, 2, 2, 1, 0	dp6 + 2Ac + $2SO_3$ + 1Na
	1292.2 $[M-H]^-$, 645.6 $[M-2H]^{2-}$	1, 2, 3, 3, 1, 0, 0	dp6 + Ac + $3SO_3$
	1356 $[M-H]^-$, 677.5 $[M-2H]^{2-}$	1, 2, 3, 3, 2, 1, 0	dp6 + 2Ac + $3SO_3$ + 1Na
	1363.4 $[M-H]^-$, 681.2 $[M-2H]^{2-}$	1, 3, 4, 0, 0, 0, 1	dp8 + $1NH_3$
	1389.4 $[M-H]^-$, 694.2 $[M-2H]^{2-}$	1, 3, 4, 0, 1, 0, 0	dp8 + Ac
	1405.4 $[M-H]^-$, 702.2 $[M-2H]^{2-}$	1, 3, 4, 0, 1, 0, 1	dp8 + Ac + $1NH_3$
27-28	1106 $[M-H]^-$, 552.6 $[M-2H]^{2-}$	1, 2, 3, 1, 0, 0, 1	dp6 + $1SO_3$ + $1NH_3$
	1170.2 $[M-H]^-$, 584.6 $[M-2H]^{2-}$	1, 2, 3, 2, 0, 0, 0	dp6 + $2SO_3$
	1228.2 $[M-H]^-$, 613.6 $[M-2H]^{2-}$	1, 2, 3, 2, 1, 0, 1	dp6 + Ac + $2SO_3$ + $1NH_3$
	1250.7 $[M-H]^-$, 624.6 $[M-2H]^{2-}$	1, 2, 3, 3, 0, 0, 0	dp6 + $3SO_3$
	1347.4 $[M-H]^-$, 673.2 $[M-2H]^{2-}$	1, 3, 4, 0, 0, 0, 0	dp8
	1389.4 $[M-H]^-$, 694.2 $[M-2H]^{2-}$	1, 3, 4, 0, 1, 0, 0	dp8 + Ac

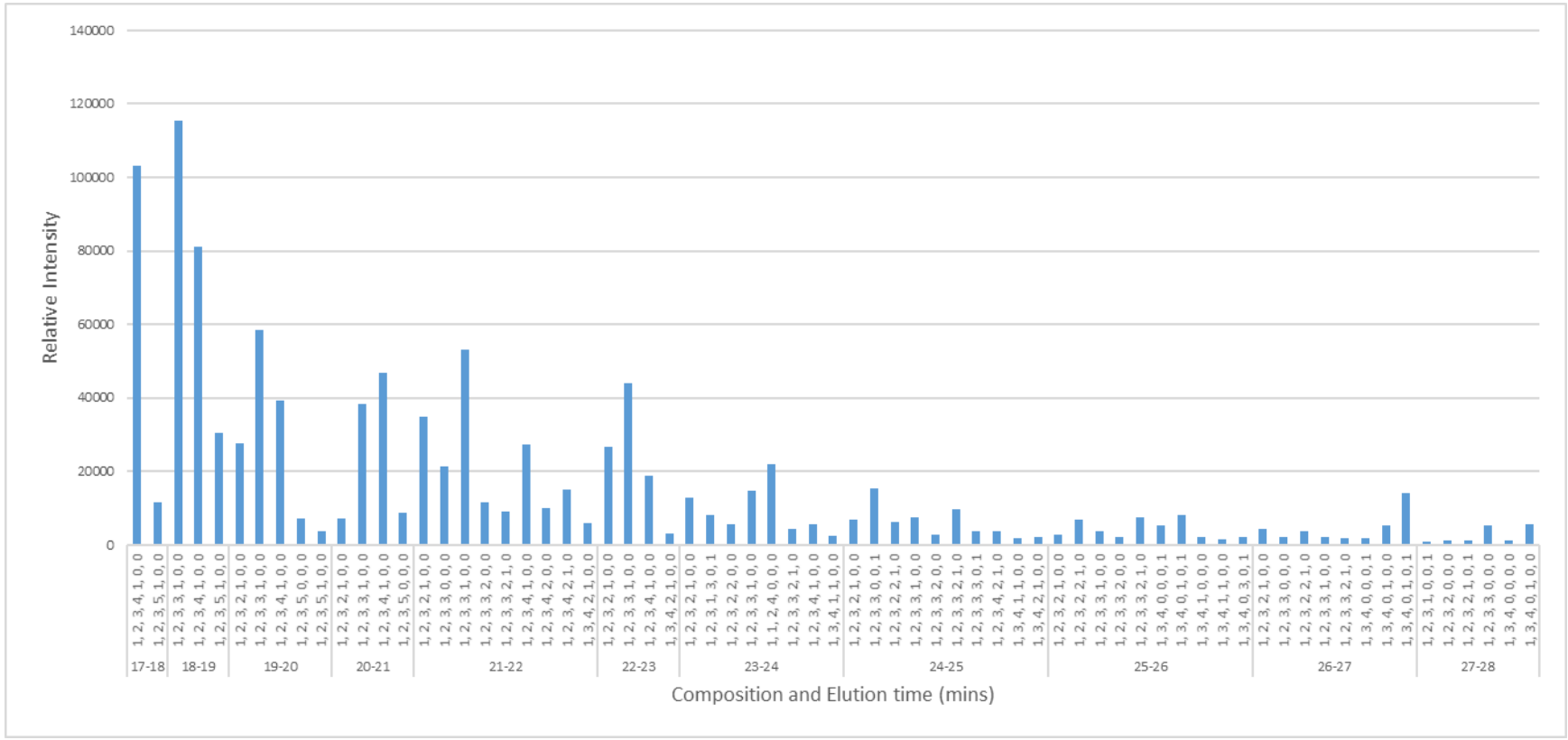

Figure S-4. Relative abundance of each oligosaccharide identified through PGC-LC-MS of SEC fraction B obtained from heparinase III digested PMHS. Compounds were identified based on MS and MS/MS spectra and placed in elution order. The oligosaccharide style is as described in Table S-1.

Table S-3. PGC LC-MS analysis of SEC fraction C obtained from heparinase III digested PMHS. Compounds were identified based on MS and MS/MS spectra and placed in elution order. The oligosaccharide style is as described in Table S-1.

Time (mins)	*m/z*	[ΔHexA, HexA, GlcN, SO_3, Ac, Na, NH_3]	Composition
17-18	1372.2 $[M-H]^-$, 685.6 $[M-2H]^{2-}$	1, 2, 3, 4, 1, 0, 0	dp6 + Ac + $4SO_3$
	1452 $[M-H]^-$, 725.5 $[M-2H]^{2-}$	1, 2, 3, 5, 1, 0, 0	dp6 + Ac + $5SO_3$
18-19	1372.2 $[M-H]^-$, 685.6 $[M-2H]^{2-}$	1, 2, 3, 4, 1, 0, 0	dp6 + Ac + $4SO_3$
	1452 $[M-H]^-$, 725.5 $[M-2H]^{2-}$	1, 2, 3, 5, 1, 0, 0	dp6 + Ac + $5SO_3$
19-20	1372.2 $[M-H]^-$, 685.6 $[M-2H]^{2-}$	1, 2, 3, 4, 1, 0, 0	dp6 + Ac + $4SO_3$
	1452 $[M-H]^-$, 725.5 $[M-2H]^{2-}$	1, 2, 3, 5, 1, 0, 0	dp6 + Ac + $5SO_3$
20-21	1372.2 $[M-H]^-$, 685.6 $[M-2H]^{2-}$	1, 2, 3, 4, 1, 0, 0	dp6 + Ac + $4SO_3$
	1292.2 $[M-H]^-$, 645.6 $[M-2H]^{2-}$	1, 2, 3, 3, 1, 0, 0	dp6 + Ac + $3SO_3$
	1330 $[M-H]^-$, 664.5 $[M-2H]^{2-}$	1, 2, 3, 4, 0, 0, 0	dp6 + $4SO_3$
	1334.2 $[M-H]^-$, 666.6 $[M-2H]^{2-}$	1, 2, 3, 3, 2, 0, 0	dp6 + 2Ac + $3SO_3$
	1410.2 $[M-H]^-$, 704.6 $[M-2H]^{2-}$	1, 2, 3, 5, 0, 0, 0	dp6 + $5SO_3$
	1414.2 $[M-H]^-$, 706.6 $[M-2H]^{2-}$	1, 2, 3, 4, 2, 0, 0	dp6 + 2Ac + $4SO_3$
	1629.2 $[M-H]^-$, 814.1 $[M-2H]^{2-}$	1, 3, 4, 3, 1, 0, 0	dp8 + Ac + $3SO_3$
	1667.2 $[M-H]^-$, 833.1 $[M-2H]^{2-}$	1, 3, 4, 4, 0, 0, 0	dp8 + $4SO_3$
	1709.2 $[M-H]^-$, 854.1 $[M-2H]^{2-}$	1, 3, 4, 4, 1, 0, 0	dp8 + Ac + $4SO_3$
21-22	1372.2 $[M-H]^-$, 685.6 $[M-2H]^{2-}$	1, 2, 3, 4, 1, 0, 0	dp6 + Ac + $4SO_3$
	1292.2 $[M-H]^-$, 645.6 $[M-2H]^{2-}$	1, 2, 3, 3, 1, 0, 0	dp6 + Ac + $3SO_3$
	1334.2 $[M-H]^-$, 666.6 $[M-2H]^{2-}$	1, 2, 3, 3, 2, 0, 0	dp6 + 2Ac + $3SO_3$
	1414.2 $[M-H]^-$, 706.6 $[M-2H]^{2-}$	1, 2, 3, 4, 2, 0, 0	dp6 + 2Ac + $4SO_3$
	1436.2 $[M-H]^-$, 717.6 $[M-2H]^{2-}$	1, 2, 3, 4, 2, 1, 0	dp6 + 2Ac + $4SO_3$ + 1Na
	1452 $[M-H]^-$, 725.5 $[M-2H]^{2-}$	1, 2, 3, 5, 1, 0, 0	dp6 + Ac + $5SO_3$
	1709.2 $[M-H]^-$, 854.1 $[M-2H]^{2-}$	1, 3, 4, 4, 1, 0, 0	dp8 + Ac + $4SO_3$
	1751.2 $[M-H]^-$, 875.1 $[M-2H]^{2-}$	1, 3, 4, 4, 2, 0, 0	dp8 + 2Ac + $4SO_3$
	1789.2 $[M-H]^-$, 894.1 $[M-2H]^{2-}$	1, 3, 4, 5, 1, 0, 0	dp8 + Ac + $5SO_3$
22-23	1292.2 $[M-H]^-$, 645.6 $[M-2H]^{2-}$	1, 2, 3, 3, 1, 0, 0	dp6 + Ac + $3SO_3$
	1414.2 $[M-H]^-$, 706.6 $[M-2H]^{2-}$	1, 2, 3, 4, 2, 0, 0	dp6 + 2Ac + $4SO_3$
	1549.4 $[M-H]^-$, 774.2 $[M-2H]^{2-}$	1, 3, 4, 2, 1, 0, 0	dp8 + Ac + $2SO_3$
	1629.2 $[M-H]^-$, 814.2 $[M-2H]^{2-}$	1, 3, 4, 3, 1, 0, 0	dp8 + Ac + $3SO_3$
	1691.2 $[M-H]^-$, 845.1 $[M-2H]^{2-}$	1, 3, 4, 2, 4, 0, 1	dp8 + 4Ac + $2SO_3$ + $1NH_3$
	1709.2 $[M-H]^-$, 854.1 $[M-2H]^{2-}$	1, 3, 4, 4, 1, 0, 0	dp8 + Ac + $4SO_3$
23-24	1292.2 $[M-H]^-$, 645.6 $[M-2H]^{2-}$	1, 2, 3, 3, 1, 0, 0	dp6 + Ac + $3SO_3$
	1330.2 $[M-H]^-$, 664.6 $[M-2H]^{2-}$	1, 2, 3, 4, 0, 0, 0	dp6 + $4SO_3$
	1352.2 $[M-H]^-$, 675.6 $[M-2H]^{2-}$	1, 2, 3, 4, 0, 1, 0	dp6 + $4SO_3$ + 1Na
	1372.2 $[M-H]^-$, 685.6 $[M-2H]^{2-}$	1, 2, 3, 4, 1, 0, 0	dp6 + Ac + $4SO_3$
	1549.4 $[M-H]^-$, 774.2 $[M-2H]^{2-}$	1, 3, 4, 2, 1, 0, 0	dp8 + Ac + $2SO_3$
	1629.2 $[M-H]^-$, 814.2 $[M-2H]^{2-}$	1, 3, 4, 3, 1, 0, 0	dp8 + Ac + $3SO_3$
24-25	1292.2 $[M-H]^-$, 645.6 $[M-2H]^{2-}$	1, 2, 3, 3, 1, 0, 0	dp6 + Ac + $3SO_3$

	1250.2 $[M-H]^-$, 624.6 $[M-2H]^{2-}$	1, 2, 3, 3, 0, 0, 0	dp6 + $3SO_3$
	1314 $[M-H]^-$, 656.5 $[M-2H]^{2-}$	1, 2, 3, 3, 1, 1, 0	dp6 + Ac + $3SO_3$ + 1Na
	1334.2 $[M-H]^-$, 666.6 $[M-2H]^{2-}$	1, 2, 3, 3, 2, 0, 0	dp6 + $2Ac$ + $3SO_3$
	1376.2 $[M-H]^-$, 687.6 $[M-2H]^{2-}$	1, 2, 3, 3, 3, 0, 0	dp6 + $3Ac$ + $3SO_3$
	1452.2 $[M-H]^-$, 725.6 $[M-2H]^{2-}$	1, 2, 3, 5, 1, 0, 0	dp6 + Ac + $5SO_3$
	1456.2 $[M-H]^-$, 727.6 $[M-2H]^{2-}$	1, 2, 3, 4, 3, 0, 0	dp6 + $3Ac$ + $4SO_3$
	1469 $[M-H]^-$, 734.2 $[M-2H]^{2-}$	1, 3, 4, 1, 1, 0, 0	dp8 + Ac + SO_3
	1507.4 $[M-H]^-$, 753.2 $[M-2H]^{2-}$	1, 3, 4, 2, 0, 0, 0	dp8 + $2SO_3$
	1587.4 $[M-H]^-$, 793.1 $[M-2H]^{2-}$	1, 3, 4, 3, 0, 0, 0	dp8 + $3SO_3$
	1629.2 $[M-H]^-$, 814.2 $[M-2H]^{2-}$	1, 3, 4, 3, 1, 0, 0	dp8 + Ac + $3SO_3$
	1633.2 $[M-H]^-$, 816.1 $[M-2H]^{2-}$	1, 3, 4, 2, 3, 0, 0	dp8 + $3Ac$ + $2SO_3$
	1667.2 $[M-H]^-$, 833.1 $[M-2H]^{2-}$	1, 3, 4, 4, 0, 0, 0	dp8 + $4SO_3$
	1709.2 $[M-H]^-$, 854.1 $[M-2H]^{2-}$	1, 3, 4, 4, 1, 0, 0	dp8 + Ac + $4SO_3$
	1793.2 $[M-H]^-$, 896.1 $[M-2H]^{2-}$	1, 3, 4, 4, 3, 0, 0	dp8 + $3Ac$ + $4SO_3$
25-26	1469.4 $[M-H]^-$, 734.2 $[M-2H]^{2-}$	1, 3, 4, 1, 1, 0, 0	dp8 + Ac + SO_3
	1485.4 $[M-H]^-$, 742.2 $[M-2H]^{2-}$	1, 3, 4, 1, 1, 0, 1	dp8 + Ac + SO_3 + $1NH_3$
	1511.4 $[M-H]^-$, 755.2 $[M-2H]^{2-}$	1, 3, 4, 1, 1, 0, 0	dp8 + Ac + $1SO_3$
	1549.4 $[M-H]^-$, 774.2 $[M-2H]^{2-}$	1, 3, 4, 2, 1, 0, 0	dp8 + Ac + $2SO_3$
	1587.4 $[M-H]^-$, 793.1 $[M-2H]^{2-}$	1, 3, 4, 3, 0, 0, 0	dp8 + $3SO_3$
	1629.2 $[M-H]^-$, 814.2 $[M-2H]^{2-}$	1, 3, 4, 3, 1, 0, 0	dp8 + Ac + $3SO_3$
	1709.2 $[M-H]^-$, 854.1 $[M-2H]^{2-}$	1, 3, 4, 4, 1, 0, 0	dp8 + Ac + $4SO_3$
27-28	1389 $[M-H]^-$, 694.2 $[M-2H]^{2-}$	1, 3, 4, 0, 1, 0, 0	dp8 + Ac
	1507.4 $[M-H]^-$, 753.2 $[M-2H]^{2-}$	1, 3, 4, 2, 0, 0, 0	dp8 + $2SO_3$
	1675.2 $[M-H]^-$, 837.1 $[M-2H]^{2-}$	1, 3, 4, 2, 4, 0, 0	dp8 + $4Ac$ + $2SO_3$
28-29	1447.2 $[M-H]^-$, 723.2 $[M-2H]^{2-}$	1, 3, 4, 0, 2, 0, 1	dp8 + $2Ac$ + $1NH_3$
	1469.4 $[M-H]^-$, 734.2 $[M-2H]^{2-}$	1, 3, 4, 1, 1, 0, 0	dp8 + Ac + SO_3
	1507.4 $[M-H]^-$, 753.2 $[M-2H]^{2-}$	1, 3, 4, 2, 0, 0, 0	dp8 + $2SO_3$
29-30	1447.2 $[M-H]^-$, 723.2 $[M-2H]^{2-}$	1, 3, 4, 0, 2, 0, 1	dp8 + $2Ac$ + $1NH_3$
	1507.4 $[M-H]^-$, 753.2 $[M-2H]^{2-}$	1, 3, 4, 2, 0, 0, 0	dp8 + $2SO_3$
	1565.4 $[M-H]^-$, 782.2 $[M-2H]^{2-}$	1, 3, 4, 2, 1, 0, 1	dp8 + Ac + $2SO_3$ + $1NH_3$
30-31	1427 $[M-H]^-$, 721.2 $[M-2H]^{2-}$	1, 3, 4, 1, 0, 0, 1	dp8 + $1SO_3$ + $1NH_3$
	1427.4 $[M-H]^-$, 732.2 $[M-2H]^{2-}$	1, 3, 4, 1, 0, 1, 1	dp8 + $1SO_3$ + $1NH_3$ + 1Na
	1485.4 $[M-H]^-$, 742.2 $[M-2H]^{2-}$	1, 3, 4, 1, 0, 0, 1	dp8 + Ac + $1SO_3$ + $1NH_3$
	1507.4 $[M-H]^-$, 753.2 $[M-2H]^{2-}$	1, 3, 4, 2, 0, 0, 0	dp8 + $2SO_3$
	1523.4 $[M-H]^-$, 761.2 $[M-2H]^{2-}$	1, 3, 4, 2, 0, 0, 1	dp8 + $2SO_3$ + $1NH_3$
	1565.4 $[M-H]^-$, 782.2 $[M-2H]^{2-}$	1, 3, 4, 2, 1, 0, 1	dp8 + Ac + $2SO_3$ + $1NH_3$
31-32	1347.4 $[M-H]^-$, 681.2 $[M-2H]^{2-}$	1, 3, 4, 0, 0, 0, 0	dp8
	1405.4 $[M-H]^-$, 702.2 $[M-2H]^{2-}$	1, 3, 4, 0, 1, 0, 1	dp8 + Ac + $1NH_3$
	1427 $[M-H]^-$, 721.2 $[M-2H]^{2-}$	1, 3, 4, 1, 0, 0, 1	dp8 + $1SO_3$ + $1NH_3$
	1523.4 $[M-H]^-$, 761.2 $[M-2H]^{2-}$	1, 3, 4, 2, 0, 0, 1	dp8 + $2SO_3$ + $1NH_3$
	1565.4 $[M-H]^-$, 782.2 $[M-2H]^{2-}$	1, 3, 4, 2, 1, 0, 1	dp8 + Ac + $2SO_3$ + $1NH_3$

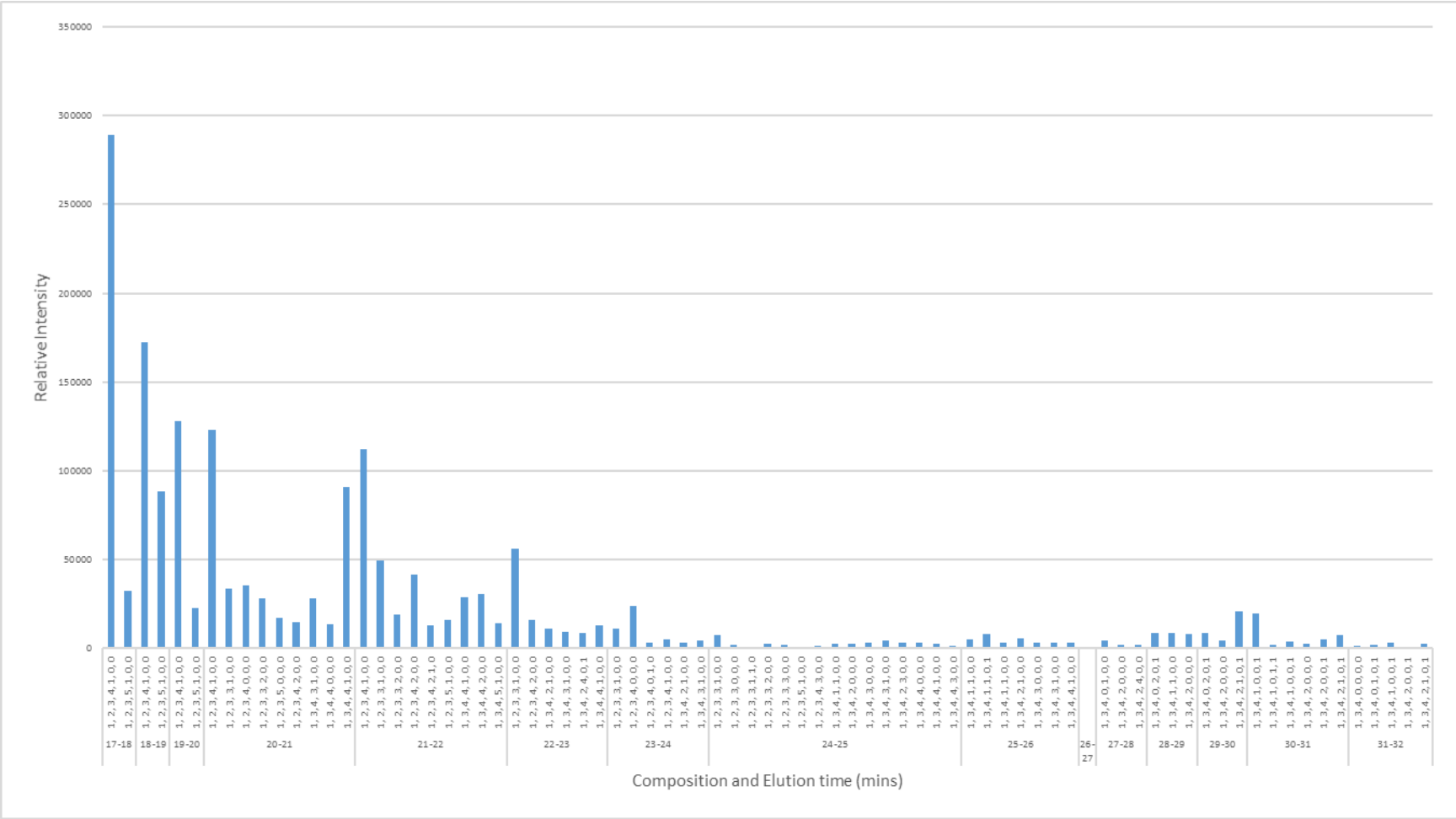

Figure S-5. Relative abundance of each oligosaccharide identified through PGC-LC-MS of SEC fraction C obtained from heparinase III digested PMHS. Compounds were identified based on MS and MS/MS spectra and placed in elution order. The oligosaccharide style is as described in Table S-1.

Table S-4. PGC LC-MS analysis of SEC fraction M obtained from heparinase III digested PMHS. Compounds were identified based on MS and MS/MS spectra and placed in elution order. The oligosaccharide style is as described in Table S-1.

Time (min)	*m/z*	[ΔHexA, HexA, GlcN, SO_3, Ac, Na, NH_3]	Composition
16-17	592.1 $[M-H]^-$	1, 1, 1, 1, 0, 0, 0	dp3 + $1SO_3$
	599.3 $[M-H]^-$	0, 1, 2, 1, 0, 1, 0	GlcN-Ido-GlcN + $1SO_3$ + 1Na
	608.1 $[M-H]^-$	1, 1, 1, 1, 0, 0, 1	dp3 + $1SO_3$ + $1NH_3$
17-18	458.1 $[M-H]^-$	1, 0, 1, 1, 1, 0, 0	dp2 + 1Ac + $1SO_3$
	592.1 $[M-H]^-$	1, 1, 1, 1, 0, 0, 0	dp3 + $1SO_3$
18-19	458.1 $[M-H]^-$	1, 0, 1, 1, 1, 0, 0	dp2 + 1Ac + $1SO_3$
	515.1 $[M-H]^-$	0, 1, 2, 0, 0, 0, 0	GlcN-Ido-GlcN
	554.1 $[M-H]^-$	1, 0, 1, 2, 1, 0, 1	dp2 + 1Ac + $2SO_3$ + $1NH_3$
19-20	458.1 $[M-H]^-$	1, 0, 1, 1, 1, 0, 0	dp2 + 1Ac + $1SO_3$
	515.1 $[M-H]^-$	0, 1, 2, 0, 0, 0, 0	GlcN-Ido-GlcN
20-21	458.1 $[M-H]^-$	1, 0, 1, 1, 1, 0, 0	dp2 + 1Ac + $1SO_3$
21-22	458.1 $[M-H]^-$	1, 0, 1, 1, 1, 0, 0	dp2 + 1Ac + $1SO_3$
22-23	458.1 $[M-H]^-$	1, 0, 1, 1, 1, 0, 0	dp2 + 1Ac + $1SO_3$
23-24	458.1 $[M-H]^-$	1, 0, 1, 1, 1, 0, 0	dp2 + 1Ac + $1SO_3$
	476.1 $[M-H]^-$	1, 0, 1, 1, 1, 0, 0	dp2 + 1Ac + $1SO_3$
	497.1 $[M-H]^-$	0, 1, 2, 0, 0, 0, 0	GlcN-Ido-GlcN
	673.3 $[M-H]^-$	1, 1, 2, 0, 0, 0, 0	dp4
	715.3 $[M-H]^-$	1, 1, 1, 2, 1, 0, 1	dp3 + 1Ac + $2SO_3$ + $1NH_3$
24-25	497.1 $[M-H]^-$	0, 1, 2, 0, 0, 0, 0	GlcN-Ido-GlcN
	673.3 $[M-H]^-$	1, 1, 2, 0, 0, 0, 0	dp4
	715.3 $[M-H]^-$	1, 1, 1, 2, 1, 0, 1	dp3 + 1Ac + $2SO_3$ + $1NH_3$
	753.2 $[M-H]^-$	1, 1, 2, 1, 0, 0, 0	dp4 + $1SO_3$

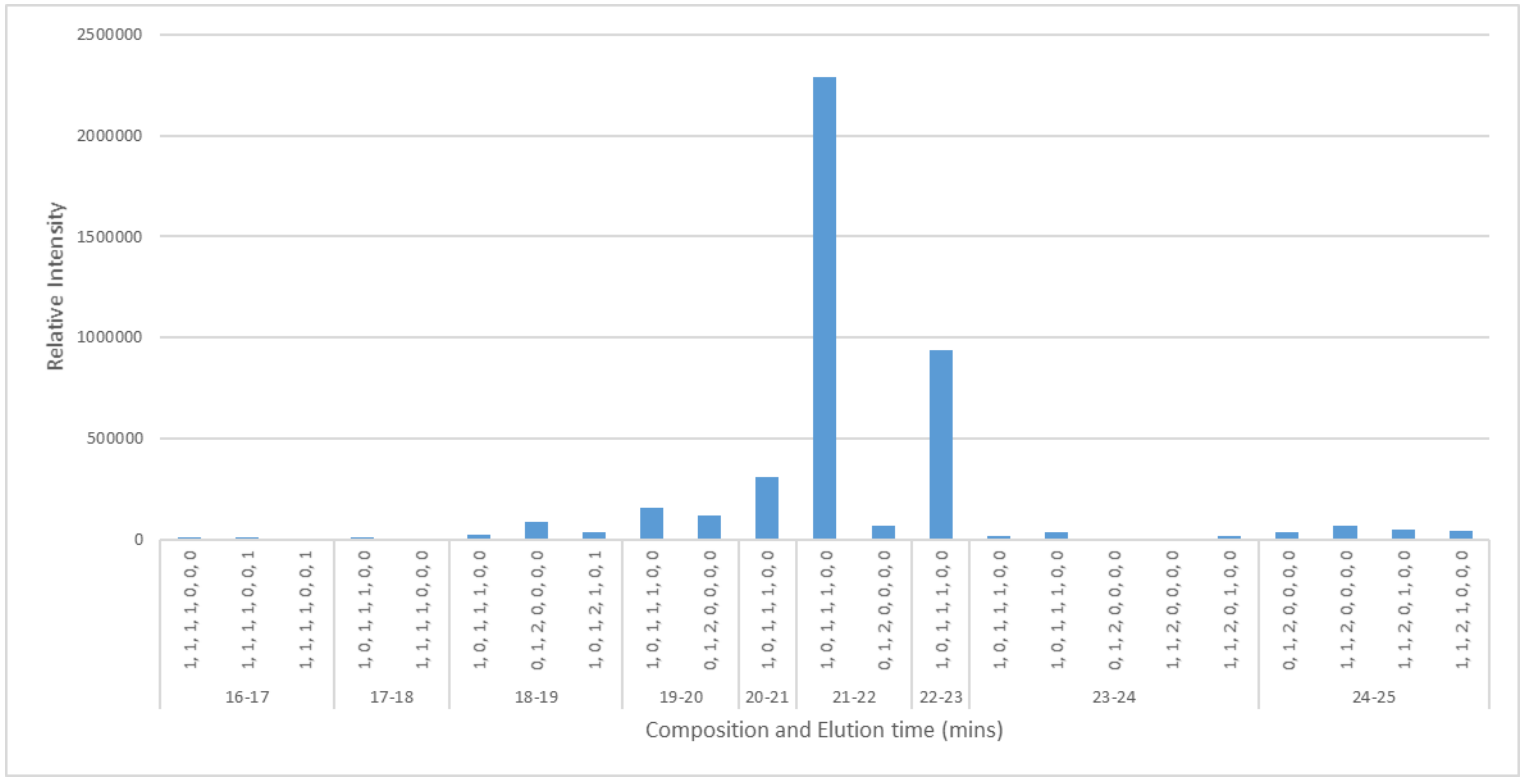

Figure S-6. Relative abundance of each oligosaccharide identified through PGC-LC-MS of SEC fraction M obtained from heparinase III digested PMHS. Compounds were identified based on MS and MS/MS spectra and placed in elution order. The oligosaccharide style is as described in Table S-1.

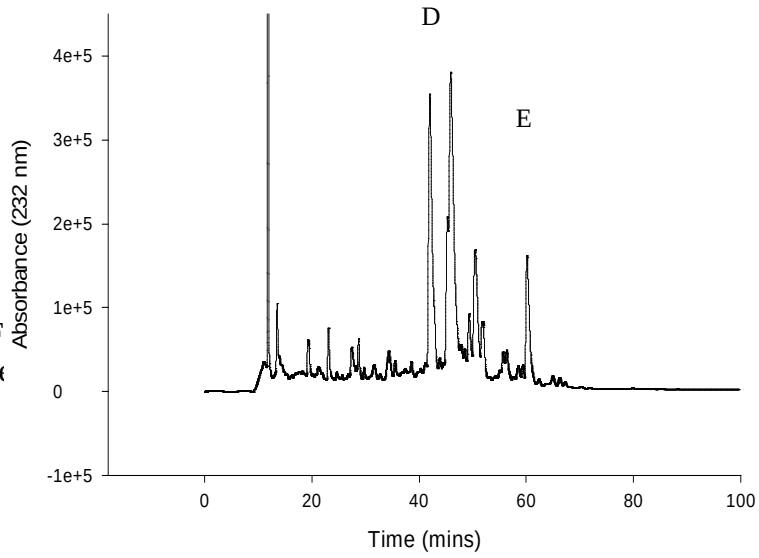

F HPLC. Peaks D and E were
s ral sequence and purity.

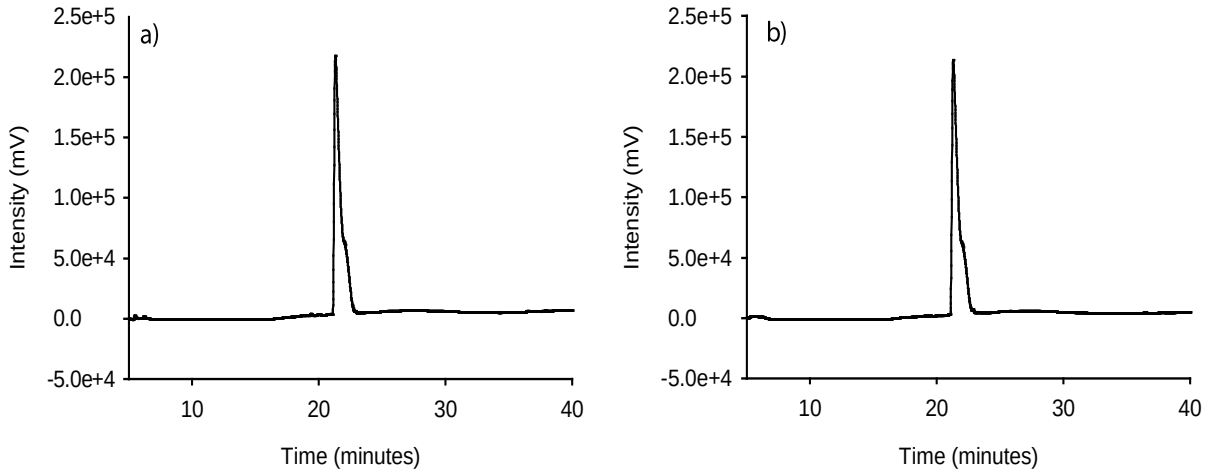

Figure S-8. Yields obtained from PGC column using a dp6 + $8SO_3$ purified heparin oligosaccharide. a) 4µg of dp6 + $8SO_3$ in water was loaded onto an analytical PGC column, the sample from 20 – 23 minutes was collected. b) The collected dp6 + $8SO_3$ was dried by centrifugal evaporation down to 200 µl to remove any acetronitrile and ammonium bicarbonate. The sample was further diluted in ddH_20 and reloaded onto the graphite column to calculate the peak area, resulting in a yield of 96%.

Table S-5: A table representation of the B, Y, C and Z ions theoretically identified from one glyosidic bond cleavage in the oligosaccharide structure ΔUA - GlcNS - UA - GlcNAc.

		1-	2-	Peak F	Peak G
B1	158.02	157.01	78.00	x	x
B2	399.04	398.03	198.51	x	x
B3	575.07	574.06	286.53	✓	x
Y1	221.09	220.08	109.54	x	x
Y2	397.12	396.11	197.55	✓	x
Y3	638.14	637.13	318.06	✓	✓
C1	176.03	175.02	87.01	x	x
C2	417.05	416.04	207.52	✓	✓
C3	593.08	592.07	295.53	✓	x
Z1	203.07	202.06	100.53	x	x
Z2	379.11	378.10	188.55	✓	✓
Z3	620.13	619.12	309.06	✓	x

Table S-6: A table representation of the B, Y, C and Z ions theoretically identified from one glyosidic bond cleavage in the oligosaccharide structure ΔUA - GlcNAc - UA - GlcNS.

		1-	2-	Peak F	Peak G
B1	158.02	157.01	78.00	x	x
B2	361.10	360.09	179.54	x	x
B3	537.13	536.12	267.56	x	✓
Y1	259.03	258.02	128.51	x	✓
Y2	435.06	434.05	216.52	x	✓
Y3	638.14	637.13	318.06	✓	✓
C1	176.00	174.99	86.99	x	x
C2	379.11	378.10	188.55	✓	✓
C3	555.14	554.13	276.56	x	✓
Z1	241.02	240.02	119.51	x	✓
Z2	417.05	416.04	207.52	✓	✓
Z3	620.13	619.12	309.06	✓	x

Table S-7: A table representation of the B, Y, C and Z ions theoretically identified from one glyosidic bond cleavage in the oligosaccharide structure ΔUA - GlcNS - UA2S - GlcNAc6S (peak H).

		1-	2-	Peak H
B1	158.02	157.01	78.00	✓
B2	399.04	398.03	198.51	✓
B3	655.03	654.02	326.51	✓
C1	176.03	175.02	87.01	x
C2	417.05	416.04	207.52	✓
C3	673.04	672.03	335.51	x
Y1	301.04	300.03	149.51	✓
Y2	557.03	556.02	277.51	x
Y3	798.06	797.05	398.02	x
Z1	283.03	282.02	140.51	✓
Z2	539.02	538.01	268.50	✓
Z3	780.05	779.04	389.02	✓

Table S-8: A table representation of the B, Y, C and Z ions theoretically identified from one glyosidic bond cleavage in the oligosaccharide structure ΔUA2S - GlcNS - UA - GlcNAc6S (peak H).

		1-	2-	Peak H
B1	237.97	236.96	117.98	x
B2	479.00	477.99	238.49	x
B3	655.03	654.02	326.51	✓
C1	255.98	254.97	126.98	✓
C2	497.01	496.00	247.50	x
C3	673.04	672.03	335.51	x
Y1	301.04	300.03	149.51	✓
Y2	477.07	476.06	237.53	x
Y3	718.10	717.09	358.04	x
Z1	283.03	282.02	140.51	✓
Z2	459.06	458.05	228.52	✓
Z3	700.09	699.08	349.04	x

Table S-9: A table representation of the B, Y, C and Z ions theoretically identified from one glyosidic bond cleavage in the oligosaccharide structure ΔUA - GlcNS6S - UA - GlcNAc6S (peak H).

		1-	2-	Peak H
B1	158.02	157.01	78.00	✓
B2	479.00	477.99	238.49	x
B3	655.03	654.02	326.51	✓
C1	176.03	175.02	87.01	x
C2	497.01	496.00	247.50	x
C3	673.04	672.03	335.51	x
Y1	301.04	300.03	149.51	✓
Y2	477.07	476.06	237.53	x
Y3	798.06	797.05	398.02	x
Z1	283.03	282.02	140.51	✓
Z2	459.06	458.05	228.52	✓
Z3	780.05	779.04	389.02	✓

Table S-10: A table representation of the B, Y, C and Z ions theoretically identified from one glyosidic bond cleavage in the oligosaccharide structure ΔUA - GlcNS6S - UA2S - GlcNAc (peak H).

		1-	2-	Peak H
B1	158.02	157.01	78.00	✓
B2	479.00	477.99	238.49	x
B3	734.99	733.98	366.49	x
C1	176.03	175.02	87.01	x
C2	497.01	496.00	247.50	x
C3	753.00	751.99	375.49	x
Y1	221.09	220.08	109.54	x
Y2	477.07	476.06	237.53	x
Y3	798.06	797.05	398.02	x
Z1	203.07	202.06	100.53	x
Z2	459.06	458.05	228.52	✓
Z3	780.05	779.04	389.02	✓

Table S-11: A table representation of the B, Y, C and Z ions theoretically identified from one glyosidic bond cleavage in the oligosaccharide structure ΔUA2S - GlcNS - UA2S - GlcNAc (peak H).

		1-	2-	Peak H
B1	237.97	236.96	117.98	x
B2	479.00	477.99	238.49	x
B3	734.99	733.98	366.49	x
C1	255.98	254.97	126.98	✓
C2	497.01	496.00	247.50	x
C3	753.00	751.99	375.49	x
Y1	221.09	220.08	109.54	x
Y2	477.07	476.06	237.53	x
Y3	718.10	717.09	358.04	x
Z1	203.07	202.06	100.53	x
Z2	459.06	458.05	228.52	✓
Z3	700.09	699.08	349.04	x

Table S-12: A table representation of the B, Y, C and Z ions theoretically identified from one glyosidic bond cleavage in the oligosaccharide structure ΔUA2S - GlcNS6S - UA - GlcNAc (peak H).

		1-	2-	Peak H
B1	237.97	236.96	117.98	x
B2	558.96	557.95	278.47	x
B3	734.99	733.98	366.49	x
C1	255.98	254.97	126.98	✓
C2	576.97	575.96	287.48	x
C3	753.00	751.99	375.49	x
Y1	221.09	220.08	109.54	x
Y2	397.12	396.11	197.55	✓
Y3	718.10	717.09	358.04	x
Z1	203.07	202.06	100.53	x
Z2	379.11	378.10	188.55	x
Z3	700.09	699.08	349.04	x

Table S-13: A table representation of the B, Y, C and Z ions theoretically identified from one glyosidic bond cleavage in the oligosaccharide structure ΔUA - GlcNAc - UA2S - GlcNS6S (peak H).

		1-	2-	Peak H
B1	158.02	157.01	78.00	✓
B2	361.10	360.09	179.54	x
B3	617.08	616.07	307.53	x
C1	176.03	175.02	87.01	x
C2	379.11	378.10	188.55	x
C3	635.10	634.09	316.54	x
Y1	338.99	337.98	168.49	✓
Y2	594.98	593.97	296.48	x
Y3	798.06	797.05	398.02	x
Z1	320.98	319.97	159.48	x
Z2	576.97	575.96	287.48	x
Z3	780.05	779.04	389.02	✓

Table S-14: A table representation of the B, Y, C and Z ions theoretically identified from one glyosidic bond cleavage in the oligosaccharide structure ΔUA - GlcNAc6S - UA - GlcNS6S (peak H).

		1-	2-	Peak H
B1	158.02	157.01	78.00	✓
B2	441.05	440.04	179.54	x
B3	617.08	616.07	307.53	x
C1	176.03	175.02	87.01	x
C2	459.06	458.05	188.55	✓
C3	635.10	634.09	316.54	x
Y1	338.99	337.98	168.49	✓
Y2	515.02	514.01	296.48	x
Y3	798.06	797.05	398.02	x
Z1	320.98	319.97	159.48	x
Z2	497.01	496.00	287.48	x
Z3	780.05	779.04	389.02	✓

Table S-15: A table representation of the B, Y, C and Z ions theoretically identified from one glyosidic bond cleavage in the oligosaccharide structure ΔUA2S - GlcNAc - UA - GlcNS6S (peak H).

		1-	2-	Peak H
B1	237.97	236.96	117.98	x
B2	441.05	440.04	219.52	x
B3	617.08	616.07	307.53	x
C1	255.98	254.97	126.98	✓
C2	459.06	458.05	228.52	✓
C3	635.10	634.09	316.54	x
Y1	338.99	337.98	168.49	✓
Y2	515.02	514.01	256.50	x
Y3	718.10	717.09	358.04	x
Z1	320.98	319.97	159.48	x
Z2	497.01	496.00	247.50	x
Z3	700.09	699.08	349.04	x

Table S-16: A table representation of the B, Y, C and Z ions theoretically identified from one glyosidic bond cleavage in the oligosaccharide structure ΔUA2S - GlcNAc - UA2S - GlcNS (peak H).

		1-	2-	Peak H
B1	237.97	236.96	117.98	x
B2	441.05	440.04	219.52	x
B3	697.04	696.03	347.51	x
C1	255.98	254.97	126.98	✓
C2	459.06	458.05	228.52	✓
C3	715.05	714.04	356.52	x
Y1	259.03	258.02	128.51	x
Y2	515.02	514.01	256.50	x
Y3	718.10	717.09	358.04	x
Z1	241.02	240.01	119.50	x
Z2	497.01	496.00	247.50	x
Z3	700.09	699.08	349.04	x

Table S-17: A table representation of the B, Y, C and Z ions theoretically identified from one glyosidic bond cleavage in the oligosaccharide structure ΔUA - GlcNAc6S - UA2S - GlcNS (peak H).

		1-	2-	Peak H
B1	158.02	157.01	78.00	✓
B2	441.05	440.04	219.52	x
B3	697.04	696.03	347.51	x
C1	176.03	175.02	87.01	x
C2	459.06	458.05	228.52	✓
C3	715.05	714.04	356.52	x
Y1	259.03	258.02	128.51	x
Y2	515.02	514.01	256.50	x
Y3	798.06	797.05	398.02	x
Z1	241.02	240.01	119.50	x
Z2	497.01	496.00	247.50	x
Z3	780.05	779.04	389.02	✓

Table S-18: A table representation of the B, Y, C and Z ions theoretically identified from one glyosidic bond cleavage in the oligosaccharide structure ΔUA2S - GlcNAc6S - UA - GlcNS (peak H).

		1-	2-	Peak H
B1	237.97	236.96	117.98	x
B2	521.01	520.00	259.50	x
B3	697.04	696.03	347.51	x
C1	255.98	254.97	126.98	✓
C2	539.02	538.01	268.50	✓
C3	715.05	714.04	356.52	x
Y1	259.03	258.02	128.51	x
Y2	435.06	434.05	216.52	x
Y3	718.10	717.09	358.04	x
Z1	241.02	240.01	119.50	x
Z2	417.05	416.04	207.52	✓
Z3	700.09	699.08	349.04	x

Table S-19: A table representation of the B, Y, C and Z ions theoretically identified from one glyosidic bond cleavage in the oligosaccharide structure ΔUA2S - GlcNS - UA - GlcNS - UA – GlcNAc.

		1-	2-	18 mins	20 mins	21 mins	22 mins
B1	237.97	236.96	117.99	x	x	x	✓
B2	479.00	477.99	238.50	✓	x	x	x
B3	655.03	654.02	326.52	x	x	x	x
B4	896.06	895.05	447.03	✓	x	x	x
B5	1072.09	1071.08	535.05	x	x	x	x
C1	255.98	254.97	126.99	x	x	x	x
C2	497.01	496.00	247.51	✓	✓	✓	✓
C3	673.04	672.03	335.52	x	x	x	x
C4	914.07	913.06	456.04	x	x	x	x
C5	1090.10	1089.09	544.05	x	x	x	x
Y1	221.09	220.08	109.55	x	x	x	x
Y2	397.12	396.11	197.56	✓	x	✓	✓
Y3	638.14	637.13	318.07	✓	✓	x	x
Y4	814.17	813.16	406.09	✓	x	✓	✓
Y5	1055.20	1054.19	526.60	✓	✓	x	✓
Z1	203.07	202.06	100.54	x	x	x	x
Z2	379.11	378.10	188.56	✓	✓	✓	x
Z3	620.13	619.12	309.07	x	✓	✓	x
Z4	796.16	795.15	397.08	x	x	✓	✓
Z5	1037.19	1036.18	517.60	x	✓	x	x
			Total B, Y C and Z fragments	8.00	6.00	6.00	6.00

Table S-20: A table representation of the B, Y, C and Z ions theoretically identified from one glyosidic bond cleavage in the oligosaccharide structure ΔUA - GlcNS6S - UA - GlcNS - UA – GlcNAc

		1-	2-	18 mins	20 mins	21 mins	22 mins
B1	158.02	157.01	78.01	x	x	x	x
B2	479.00	477.99	238.50	✓	x	x	x
B3	655.03	654.02	326.52	x	x	x	x
B4	896.06	895.05	447.03	✓	x	x	x
B5	1072.09	1071.08	535.05	x	x	x	x
C1	176.03	175.02	87.02	x	x	x	x
C2	497.01	496.00	247.51	✓	✓	✓	✓
C3	673.04	672.03	335.52	x	x	x	x
C4	914.07	913.06	456.04	x	x	x	x
C5	1090.10	1089.09	544.05	x	x	x	x
Y1	221.09	220.08	109.55	x	x	x	x
Y2	397.12	396.11	197.56	✓	x	✓	✓
Y3	638.14	637.13	318.07	✓	✓	x	x
Y4	814.17	813.16	406.09	✓	x	✓	✓
Y5	1135.16	1134.15	566.58	x	x	x	x
Z1	203.07	202.06	100.54	x	x	x	x
Z2	379.11	378.10	188.56	✓	✓	✓	x
Z3	620.13	619.12	309.07	x	✓	✓	x
Z4	796.16	795.15	397.08	x	x	✓	✓
Z5	1117.15	1116.14	557.58	x	x	x	x
			Total B, Y C and Z fragments	7.00	4.00	6.00	4.00

Table S-21: A table representation of the B, Y, C and Z ions theoretically identified from one glyosidic bond cleavage in the oligosaccharide structure ΔUA - GlcNS - UA2S - GlcNS - UA – GlcNAc.

		1-	2-	18 mins	20 mins	21 mins	22 mins
B1	158.02	157.01	78.01	x	x	x	x
B2	399.04	398.03	198.52	x	✓	x	x
B3	655.03	654.02	326.52	x	x	x	x
B4	896.06	895.05	447.03	x	x	x	x
B5	1072.09	1071.08	535.05	x	x	x	x
C1	176.03	175.02	87.02	x	x	x	x
C2	417.05	416.04	207.53	✓	✓	x	✓
C3	673.04	672.03	335.52	x	x	x	x
C4	914.07	913.06	456.04	x	x	x	x
C5	1090.10	1089.09	544.05	x	x	x	x
Y1	221.09	220.08	109.55	x	x	x	x
Y2	397.12	396.11	197.56	✓	x	✓	✓
Y3	638.14	637.13	318.07	✓	✓	x	x
Y4	894.13	893.12	446.07	x	x	x	x
Y5	1135.16	1134.15	566.58	x	x	x	x
Z1	203.07	202.06	100.54	x	x	x	x
Z2	379.11	378.10	188.56	✓	✓	✓	x
Z3	620.13	619.12	309.07	x	✓	✓	x
Z4	876.12	875.11	437.06	x	x	x	x
Z5	1117.15	1116.14	557.58	x	x	x	x
			Total B, Y C and Z fragments	4.00	5.00	3.00	2.00

Table S-22: A table representation of the B, Y, C and Z ions theoretically identified from one glyosidic bond cleavage in the oligosaccharide structure ΔUA - GlcNS - UA - GlcNS6S - UA - GlcNAc.

		1-	2-	18 mins	20 mins	21 mins	22 mins
B1	158.02	157.01	78.01	x	x	x	x
B2	399.04	398.03	198.52	x	x	x	x
B3	575.07	574.06	286.54	x	x	x	✓
B4	896.06	895.05	447.03	✓	x	x	x
B5	1072.09	1071.08	535.05	x	x	x	x
C1	176.03	175.02	87.02	x	x	x	x
C2	417.05	416.04	207.53	✓	✓	x	✓
C3	593.08	592.07	295.54	x	x	x	✓
C4	914.07	913.06	456.04	x	x	x	x
C5	1090.10	1089.09	544.05	x	x	x	x
Y1	221.09	220.08	109.55	x	x	x	x
Y2	397.12	396.11	197.56	✓	x	✓	✓
Y3	718.10	717.09	358.05	✓	x	✓	✓
Y4	894.13	893.12	446.07	x	x	x	x
Y5	1135.16	1134.15	566.58	x	x	x	x
Z1	203.07	202.06	100.54	x	x	x	x
Z2	379.11	378.10	188.56	✓	✓	✓	x
Z3	700.09	699.08	349.05	x	x	x	x
Z4	876.12	875.11	437.06	x	x	x	x
Z5	1117.15	1116.14	557.58	x	x	x	x
			Total B, Y C and Z fragments	5.00	2.00	3.00	5.00

Table S-23: A table representation of the B, Y, C and Z ions theoretically identified from one glyosidic bond cleavage in the oligosaccharide structure ΔUA - GlcNS - UA - GlcNS - UA2S – GlcNAc.

		1-	2-	18 mins	20 mins	21 mins	22 mins
B1	158.02	157.01	78.01	x	x	x	x
B2	399.04	398.03	198.52	x	x	x	x
B3	575.07	574.06	286.54	x	x	x	✓
B4	816.10	815.09	407.05	x	x	✓	x
B5	1072.09	1071.08	535.05	x	x	x	x
C1	176.03	175.02	87.02	x	x	x	x
C2	417.05	416.04	207.53	✓	✓	x	✓
C3	593.08	592.07	295.54	x	x	x	✓
C4	834.11	833.10	416.06	x	x	x	x
C5	1090.10	1089.09	544.05	x	x	x	x
Y1	221.09	220.08	109.55	x	x	x	x
Y2	477.07	476.06	237.54	✓	✓	✓	✓
Y3	718.10	717.09	358.05	✓	x	✓	✓
Y4	894.13	893.12	446.07	x	x	x	x
Y5	1135.16	1134.15	566.58	x	x	x	x
Z1	203.07	202.06	100.54	x	x	x	x
Z2	459.06	458.05	228.53	x	x	x	x
Z3	700.09	699.08	349.05	x	x	x	x
Z4	876.12	875.11	437.06	x	x	x	x
Z5	1117.15	1116.14	557.58	x	x	x	x
			Total B, Y C and Z fragments	3.00	2.00	3.00	5.00

Table S-24: A table representation of the B, Y, C and Z ions theoretically identified from one glyosidic bond cleavage in the oligosaccharide structure ΔUA - GlcNS - UA - GlcNS - UA - GlcNAc6S.

		1-	2-	18 mins	20 mins	21 mins	22 mins
B1	158.02	157.01	78.01	x	x	x	x
B2	399.04	398.03	198.52	x	x	x	x
B3	575.07	574.06	286.54	x	x	x	✓
B4	816.10	815.09	407.05	x	x	✓	x
B5	992.13	991.12	495.07	x	✓	x	x
C1	176.03	175.02	87.02	x	x	x	x
C2	417.05	416.04	207.53	✓	✓	x	✓
C3	593.08	592.07	295.54	x	x	x	✓
C4	834.11	833.10	416.06	x	x	x	x
C5	1010.14	1009.13	504.07	x	x	x	x
Y1	301.04	300.03	149.52	x	x	x	x
Y2	477.07	476.06	237.54	✓	✓	✓	✓
Y3	718.10	717.09	358.05	✓	x	✓	✓
Y4	894.13	893.12	446.07	x	x	x	x
Y5	1135.16	1134.15	566.58	x	x	x	x
Z1	283.03	282.02	140.52	x	x	x	x
Z2	459.06	458.05	228.53	x	x	x	x
Z3	700.09	699.08	349.05	x	x	x	x
Z4	876.12	875.11	437.06	x	x	x	x
Z5	1117.15	1116.14	557.58	x	x	x	x
			Total B, Y C and Z fragments	3.00	3.00	3.00	5.00

Table S-25: A table representation of the B, Y, C and Z ions theoretically identified from one glyosidic bond cleavage in the oligosaccharide structure ΔUA2S - GlcNS - UA - GlcNAc - UA - GlcNS.

		1-	2-	18 mins	20 mins	21 mins	22 mins
B1	237.97	236.96	117.99	x	x	x	✓
B2	479.00	477.99	238.50	x	x	x	x
B3	655.03	654.02	326.52	x	x	x	x
B4	858.11	857.10	428.06	x	x	x	x
B5	1034.14	1033.13	516.07	x	x	x	x
C1	255.98	254.97	126.99	x	x	x	x
C2	497.01	496.00	247.51	✓	✓	✓	✓
C3	673.04	672.03	335.52	x	x	x	x
C4	876.12	875.11	437.06	x	x	x	x
C5	1052.15	1051.14	525.08	x	x	x	x
Y1	259.03	258.02	128.52	x	x	x	x
Y2	435.06	434.05	216.53	x	x	x	x
Y3	638.14	637.13	318.07	✓	✓	x	x
Y4	814.17	813.16	406.09	✓	x	✓	✓
Y5	1055.20	1054.19	526.60	✓	✓	x	✓
Z1	241.02	240.01	119.51	x	x	x	x
Z2	417.05	416.04	207.53	✓	✓	x	✓
Z3	620.13	619.12	309.07	x	✓	✓	x
Z4	796.16	795.15	397.08	x	x	✓	✓
Z5	1037.19	1036.18	517.60	x	✓	x	x
			Total B, Y C and Z fragments	5.00	6.00	4.00	6.00

Table S-26: A table representation of the B, Y, C and Z ions theoretically identified from one glyosidic bond cleavage in the oligosaccharide structure ΔUA - GlcNS6S - UA - GlcNAc - UA - GlcNS.

		1-	2-	18 mins	20 mins	21 mins	22 mins
B1	158.02	157.01	78.01	x	x	x	x
B2	479.00	477.99	238.50	x	x	x	x
B3	655.03	654.02	326.52	x	x	x	x
B4	858.11	857.10	428.06	x	x	x	x
B5	1034.14	1033.13	516.07	x	x	x	x
C1	176.00	174.99	87.00	x	x	x	x
C2	497.01	496.00	247.51	✓	✓	✓	✓
C3	673.04	672.03	335.52	x	x	x	x
C4	876.12	875.11	437.06	x	x	x	x
C5	1052.15	1051.14	525.08	x	x	x	x
Y1	259.03	258.02	128.52	x	x	x	x
Y2	435.06	434.05	216.53	x	x	x	x
Y3	638.14	637.13	318.07	✓	✓	x	x
Y4	814.17	813.16	406.09	✓	x	✓	✓
Y5	1135.16	1134.15	566.58	x	x	x	x
Z1	241.02	240.01	119.51	x	x	x	x
Z2	417.05	416.04	207.53	✓	✓	x	✓
Z3	620.13	619.12	309.07	x	✓	✓	x
Z4	796.16	795.15	397.08	x	x	✓	✓
Z5	1117.15	1116.14	557.58	x	x	x	x
			Total B, Y C and Z fragments	4.00	4.00	4.00	4.00

Table S-27: A table representation of the B, Y, C and Z ions theoretically identified from one glyosidic bond cleavage in the oligosaccharide structure ΔUA - GlcNS - UA2S - GlcNAc - UA - GlcNS.

		1-	2-	18 mins	20 mins	21 mins	22 mins
B1	158.02	157.01	78.01	x	x	x	x
B2	399.04	398.03	198.52	x	x	x	x
B3	655.03	654.02	326.52	x	x	x	x
B4	858.11	857.10	428.06	x	x	x	x
B5	1034.14	1033.13	516.07	x	x	x	x
C1	176.03	175.02	87.02	x	x	x	x
C2	417.05	416.04	207.53	✓	✓	x	✓
C3	673.04	672.03	335.52	x	x	x	x
C4	876.12	875.11	437.06	x	x	x	x
C5	1052.15	1051.14	525.08	x	x	x	x
Y1	259.03	258.02	128.52	x	x	x	x
Y2	435.06	434.05	216.53	x	x	x	x
Y3	638.14	637.13	318.07	✓	✓	x	x
Y4	894.13	893.12	446.07	x	x	x	x
Y5	1135.16	1134.15	566.58	x	x	x	x
Z1	241.02	240.01	119.51	x	x	x	x
Z2	417.05	416.04	207.53	✓	✓	x	✓
Z3	620.13	619.12	309.07	x	✓	✓	x
Z4	876.12	875.11	437.06	x	x	x	x
Z5	1117.15	1116.14	557.58	x	x	x	x
			Total B, Y C and Z fragments	3.00	4.00	1.00	2.00

Table S-28: A table representation of the B, Y, C and Z ions theoretically identified from one glyosidic bond cleavage in the oligosaccharide structure ΔUA - GlcNS - UA - GlcNAc6S - UA - GlcNS.

		1-	2-	18 mins	20 mins	21 mins	22 mins
B1	158.02	157.01	78.01	x	x	x	x
B2	399.04	398.03	198.52	x	x	x	x
B3	575.07	574.06	286.54	x	x	x	✓
B4	858.11	857.10	428.06	x	x	x	x
B5	1034.14	1033.13	516.07	x	x	x	x
C1	176.03	175.02	87.02	x	x	x	x
C2	417.05	416.04	207.53	✓	✓	x	✓
C3	593.08	592.07	295.54	x	x	x	✓
C4	876.12	875.11	437.06	x	x	x	x
C5	1052.15	1051.14	525.08	x	x	x	x
Y1	259.03	258.02	128.52	x	x	x	x
Y2	435.06	434.05	216.53	x	x	x	x
Y3	718.10	717.09	358.05	✓	x	✓	✓
Y4	894.13	893.12	446.07	x	x	x	x
Y5	1135.16	1134.15	566.58	x	x	x	x
Z1	241.02	240.01	119.51	x	x	x	x
Z2	417.05	416.04	207.53	✓	✓	x	✓
Z3	700.09	699.08	349.05	x	x	x	x
Z4	876.12	875.11	437.06	x	x	x	x
Z5	1117.15	1116.14	557.58	x	x	x	x
			Total B, Y C and Z fragments	3.00	2.00	1.00	5.00

Table S-29: A table representation of the B, Y, C and Z ions theoretically identified from one glyosidic bond cleavage in the oligosaccharide structure ΔUA - GlcNS - UA - GlcNAc - UA2S - GlcNS.

		1-	2-	18 mins	20 mins	21 mins	22 mins
B1	158.02	157.01	78.01	x	x	x	x
B2	399.04	398.03	198.52	x	x	x	x
B3	575.07	574.06	286.54	x	x	x	✓
B4	778.15	777.14	388.08	x	x	x	✓
B5	1034.14	1033.13	516.07	x	x	x	x
C1	176.03	175.02	87.02	x	x	x	x
C2	417.05	416.04	207.53	✓	✓	x	✓
C3	593.08	592.07	295.54	x	x	x	✓
C4	796.16	795.15	397.08	x	x	✓	✓
C5	1052.15	1051.14	525.08	x	x	x	x
Y1	259.03	258.02	128.52	x	x	x	x
Y2	515.02	514.01	256.51	x	x	x	x
Y3	718.10	717.09	358.05	✓	x	✓	✓
Y4	894.13	893.12	446.07	x	x	x	x
Y5	1135.16	1134.15	566.58	x	x	x	x
Z1	241.02	240.01	119.51	x	x	x	x
Z2	497.01	496.00	247.51	✓	✓	✓	✓
Z3	700.09	699.08	349.05	x	x	x	x
Z4	876.12	875.11	437.06	x	x	x	x
Z5	1117.15	1116.14	557.58	x	x	x	x
			Total B, Y C and Z fragments	3.00	2.00	3.00	7.00

Table S-30: A table representation of the B, Y, C and Z ions theoretically identified from one glyosidic bond cleavage in the oligosaccharide structure ΔUA - GlcNS - UA - GlcNAc - UA - GlcNS6S.

		1-	2-	18 mins	20 mins	21 mins	22 mins
B1	158.02	157.01	78.01	x	x	x	x
B2	399.04	398.03	198.52	x	x	x	x
B3	575.07	574.06	286.54	x	x	x	✓
B4	778.15	777.14	388.08	x	x	x	✓
B5	954.19	953.18	476.10	x	x	x	✓
C1	176.03	175.02	87.02	x	x	x	x
C2	417.05	416.04	207.53	✓	✓	x	✓
C3	593.08	592.07	295.54	x	x	x	✓
C4	796.16	795.15	397.08	x	x	✓	✓
C5	972.20	971.19	485.10	x	x	x	x
Y1	338.99	337.98	168.50	x	x	x	x
Y2	515.02	514.01	256.51	x	x	x	x
Y3	718.10	717.09	358.05	✓	x	✓	✓
Y4	894.13	893.12	446.07	x	x	x	x
Y5	1135.16	1134.15	566.58	x	x	x	x
Z1	320.98	319.97	159.49	✓	x	x	x
Z2	497.01	496.00	247.51	✓	✓	✓	✓
Z3	700.09	699.08	349.05	x	x	x	x
Z4	876.12	875.11	437.06	x	x	x	x
Z5	1117.15	1116.14	557.58	x	x	x	x
			Total B, Y C and Z fragments	4.00	2.00	3.00	8.00

Table S-31: A table representation of the B, Y, C and Z ions theoretically identified from one glyosidic bond cleavage in the oligosaccharide structure ΔUA2S - GlcNAc - UA - GlcNS - UA - GlcNS.

		1-	2-	18 mins	20 mins	21 mins	22 mins
B1	237.97	236.96	117.99	x	x	x	x
B2	441.05	440.04	219.53	x	x	x	x
B3	617.08	616.07	307.54	✓	x	x	x
B4	858.11	857.10	428.06	x	x	x	x
B5	1034.14	1033.13	516.07	x	x	x	x
C1	255.98	254.97	126.99	x	x	x	x
C2	459.06	458.05	228.53	x	x	x	x
C3	635.10	634.09	316.55	x	x	x	x
C4	876.12	875.11	437.06	x	x	x	x
C5	1052.15	1051.14	525.08	x	x	x	x
Y1	259.03	258.02	128.52	x	x	x	x
Y2	435.06	434.05	216.53	x	x	x	x
Y3	676.09	675.08	337.05	x	✓	x	x
Y4	852.12	851.11	425.06	x	x	x	x
Y5	1055.20	1054.19	526.60	x	x	x	x
Z1	241.02	240.01	119.51	x	x	x	x
Z2	417.05	416.04	207.53	✓	✓	x	✓
Z3	658.08	657.07	328.04	x	x	x	x
Z4	834.11	833.10	416.06	x	x	x	x
Z5	1037.19	1036.18	517.60	x	✓	x	x
			Total B, Y C and Z fragments	2.00	3.00	0.00	1.00

Table S-32: A table representation of the B, Y, C and Z ions theoretically identified from one glyosidic bond cleavage in the oligosaccharide structure ΔUA - GlcNAc6S - UA - GlcNS - UA - GlcNS.

		1-	2-	18 mins	20 mins	21 mins	22 mins
B1	158.02	157.01	78.01	x	x	x	x
B2	441.05	440.04	219.53	x	x	x	x
B3	617.08	616.07	307.54	✓	x	x	x
B4	858.11	857.10	428.06	x	x	x	x
B5	1034.14	1033.13	516.07	x	x	x	x
C1	176.03	175.02	87.02	x	x	x	x
C2	459.06	458.05	228.53	x	x	x	x
C3	635.10	634.09	316.55	x	x	x	x
C4	876.12	875.11	437.06	x	x	x	x
C5	1052.15	1051.14	525.08	x	x	x	x
Y1	259.03	258.02	128.52	x	x	x	x
Y2	435.06	434.05	216.53	x	x	x	x
Y3	676.09	675.08	337.05	x	✓	x	x
Y4	852.12	851.11	425.06	x	x	x	x
Y5	1135.16	1134.15	566.58	x	x	x	x
Z1	241.02	240.01	119.51	x	x	x	x
Z2	417.05	416.04	207.53	✓	✓	x	✓
Z3	658.08	657.07	328.04	x	x	x	x
Z4	834.11	833.10	416.06	x	x	x	x
Z5	1117.15	1116.14	557.58	x	x	x	x
			Total B, Y C and Z fragments	2.00	2.00	0.00	1.00

Table S-33: A table representation of the B, Y, C and Z ions theoretically identified from one glyosidic bond cleavage in the oligosaccharide structure ΔUA - GlcNAc - UA2S - GlcNS - UA - GlcNS.

		1-	2-	18 mins	20 mins	21 mins	22 mins
B1	158.02	157.01	78.01	x	x	x	x
B2	361.10	360.09	179.55	x	x	x	x
B3	617.08	616.07	307.54	✓	x	x	x
B4	858.11	857.10	428.06	x	x	x	x
B5	1034.14	1033.13	516.07	x	x	x	x
C1	176.03	175.02	87.02	x	x	x	x
C2	379.11	378.10	188.56	✓	✓	✓	x
C3	635.10	634.09	316.55	x	x	x	x
C4	876.12	875.11	437.06	x	x	x	x
C5	1052.15	1051.14	525.08	x	x	x	x
Y1	259.03	258.02	128.52	x	x	x	x
Y2	435.06	434.05	216.53	x	x	x	x
Y3	676.09	675.08	337.05	x	✓	x	x
Y4	932.08	931.07	465.04	x	x	x	x
Y5	1135.16	1134.15	566.58	x	x	x	x
Z1	241.02	240.01	119.51	x	x	x	x
Z2	417.05	416.04	207.53	✓	✓	x	✓
Z3	658.08	657.07	328.04	x	x	x	x
Z4	914.07	913.06	456.04	x	x	x	x
Z5	1117.15	1116.14	557.58	x	x	x	x
			Total B, Y C and Z fragments	3.00	3.00	1.00	1.00

Table S-34: A table representation of the B, Y, C and Z ions theoretically identified from one glyosidic bond cleavage in the oligosaccharide structure ΔUA - GlcNAc - UA - GlcNS6S - UA - GlcNS.

		1-	2-	18 mins	20 mins	21 mins	22 mins
B1	158.02	157.01	78.01	x	x	x	x
B2	361.10	360.09	179.55	x	x	x	x
B3	537.13	536.12	267.57	x	x	✓	x
B4	858.11	857.10	428.06	x	x	x	x
B5	1034.14	1033.13	516.07	x	x	x	x
C1	176.03	175.02	87.02	x	x	x	x
C2	379.11	378.10	188.56	✓	✓	✓	x
C3	555.14	554.13	276.57	x	x	x	x
C4	876.12	875.11	437.06	x	x	x	x
C5	1052.15	1051.14	525.08	x	x	x	x
Y1	259.03	258.02	128.52	x	x	x	x
Y2	435.06	434.05	216.53	x	x	x	x
Y3	756.05	755.04	377.03	x	x	x	x
Y4	932.08	931.07	465.04	x	x	x	x
Y5	1135.16	1134.15	566.58	x	x	x	x
Z1	241.02	240.01	119.51	x	x	x	x
Z2	417.05	416.04	207.53	✓	✓	x	✓
Z3	738.04	737.03	368.02	x	✓	x	x
Z4	914.07	913.06	456.04	x	x	x	x
Z5	1117.15	1116.14	557.58	x	x	x	x
			Total B, Y C and Z fragments	2.00	3.00	2.00	1.00

Table S-35: A table representation of the B, Y, C and Z ions theoretically identified from one glyosidic bond cleavage in the oligosaccharide structure ΔUA - GlcNAc - UA - GlcNS - UA2S - GlcNS.

		1-	2-	18 mins	20 mins	21 mins	22 mins
B1	158.02	157.01	78.01	x	x	x	x
B2	361.10	360.09	179.55	x	x	x	x
B3	537.13	536.12	267.57	x	x	✓	x
B4	778.15	777.14	388.08	x	x	x	✓
B5	1034.14	1033.13	516.07	x	x	x	x
C1	176.03	175.02	87.02	x	x	x	x
C2	379.11	378.10	188.56	✓	✓	✓	x
C3	555.14	554.13	276.57	x	x	x	x
C4	796.16	795.15	397.08	x	x	x	x
C5	1052.15	1051.14	525.08	x	x	✓	x
Y1	259.03	258.02	128.52	x	x	x	x
Y2	515.02	514.01	256.51	x	x	x	x
Y3	756.05	755.04	377.03	x	x	x	x
Y4	932.08	931.07	465.04	x	x	x	x
Y5	1135.16	1134.15	566.58	x	x	x	x
Z1	241.02	240.01	119.51	x	x	x	x
Z2	497.01	496.00	247.51	✓	✓	✓	✓
Z3	738.04	737.03	368.02	x	✓	x	x
Z4	914.07	913.06	456.04	x	x	x	x
Z5	1117.15	1116.14	557.58	x	x	x	x
			Total B, Y C and Z fragments	2.00	3.00	4.00	2.00

Table S-36: A table representation of the B, Y, C and Z ions theoretically identified from one glyosidic bond cleavage in the oligosaccharide structure ΔUA - GlcNAc - UA - GlcNS - UA - GlcNS6S.

		1-	2-	18 mins	20 mins	21 mins	22 mins
B1	158.02	157.01	78.01	x	x	x	x
B2	361.10	360.09	179.55	x	x	x	x
B3	537.13	536.12	267.57	x	x	✓	x
B4	778.15	777.14	388.08	x	x	x	✓
B5	954.19	953.18	476.10	x	x	x	✓
C1	176.03	175.02	87.02	x	x	x	x
C2	379.11	378.10	188.56	✓	✓	✓	x
C3	555.14	554.13	276.57	x	x	x	x
C4	796.16	795.15	397.08	x	x	x	x
C5	972.20	971.19	485.10	x	✓	x	x
Y1	338.99	337.98	168.50	x	x	x	x
Y2	515.02	514.01	256.51	x	x	x	x
Y3	756.05	755.04	377.03	x	x	x	x
Y4	932.08	931.07	465.04	x	x	x	x
Y5	1135.16	1134.15	566.58	x	x	x	x
Z1	320.98	319.97	159.49	✓	x	x	x
Z2	497.01	496.00	247.51	✓	✓	✓	✓
Z3	738.04	737.03	368.02	x	✓	x	x
Z4	914.07	913.06	456.04	x	x	x	x
Z5	1117.15	1116.14	557.58	x	x	x	x
			Total B, Y C and Z fragments	3.00	4.00	3.00	3.00

Table S-37: A table representation of the B, Y, C and Z ions theoretically identified from one glyosidic bond cleavage of all 18 oligosaccharide sequences.

	18 mins	20 mins	21 mins	22 mins
ΔUA2S - GlcNS - UA - GlcNS - UA - GlcNAc	8	6	6	6
ΔUA - GlcNS6S - UA - GlcNS - UA - GlcNAc	7	4	6	4
ΔUA - GlcNS - UA2S - GlcNS - UA - GlcNAc	4	5	3	2
ΔUA - GlcNS - UA - GlcNS6S - UA - GlcNAc	5	2	3	5
ΔUA - GlcNS - UA - GlcNS - UA2S - GlcNAc	3	2	3	5
ΔUA - GlcNS - UA - GlcNS - UA - GlcNAc6S	3	3	3	5
ΔUA2S - GlcNS - UA - GlcNAc - UA - GlcNS	5	6	4	6
ΔUA - GlcNS6S - UA - GlcNAc - UA - GlcNS	4	4	4	4
ΔUA - GlcNS - UA2S - GlcNAc - UA - GlcNS	3	4	1	2
ΔUA - GlcNS - UA - GlcNAc6S - UA - GlcNS	3	2	1	5
ΔUA - GlcNS - UA - GlcNAc - UA2S - GlcNS	3	2	3	7
ΔUA - GlcNS - UA - GlcNAc - UA - GlcNS6S	4	2	3	8
ΔUA2S - GlcNAc - UA - GlcNS - UA - GlcNS	2	3	0	1
ΔUA - GlcNAc6S - UA - GlcNS - UA - GlcNS	2	2	0	1
ΔUA - GlcNAc - UA2S - GlcNS - UA - GlcNS	3	3	1	1
ΔUA - GlcNAc - UA - GlcNS6S - UA - GlcNS	2	3	2	1
ΔUA - GlcNAc - UA - GlcNS - UA2S - GlcNS	2	3	4	2
ΔUA - GlcNAc - UA - GlcNS - UA - GlcNS6S	3	4	3	3

Table S-38: A table representation of the B, Y, C and Z ions theoretically identified from one glyosidic bond cleavage in the oligosaccharide structure UA - GlcNS - UA (peak O).

		1-	2-	Peak O
B1	158.02	157.01	78.00	x
B2 - SO_3	319.09	318.08	158.54	✓
B2	399.04	398.03	198.51	✓
C1	176.03	175.02	87.01	✓
C2 - SO_3	337.10	336.09	167.54	✓
C2	417.05	416.04	207.52	✓
Y1	194.04	193.03	96.01	x
Y2 - SO_3	355.11	354.10	176.55	✓
Y2	435.06	434.05	216.52	✓
Z1	176.03	175.02	87.01	✓
Z2 - SO_3	337.10	336.09	167.54	✓
Z2	417.05	416.04	207.52	✓